6-29-2011

Investigation of miRNAs Expression in a Citron-Kinase Mutant Model of Microcephaly

Shan Parikh
University of Connecticut - Storrs, shansp89@gmail.com

Investigation of miRNA Expression in a Citron-Kinase Mutant Model of Microcephaly

Shan Parikh

B.S., University of Connecticut, 2010

A Thesis

Submitted in Partial Fulfillment of the

Requirements for the Degree of

Master of Science

at the

University of Connecticut

2011

APPROVAL PAGE

Master of Science Thesis

Investigation of miRNA Expression in a Citron-Kinase Mutant Model of Microcephaly

Presented by

Shan Parikh, B.S.

Major Advisor _____

Dr. Joseph LoTurco

Associate Advisor _____

Dr. Rahul Kanadia

Associate Advisor _____

Dr. Anastasios Tzingounis

University of Connecticut

2011

I want to thank my parents and my brother for supporting me through my journey in academics and specifically thank Dr. LoTurco for his continued patience and his guidance throughout my years at the University of Connecticut.

Table of Contents

Abstract

Mutation of Citron-Kinase (Cit-K) in rodents causes substantial reductions in the number of neurons generated in the CNS and results in a primary microcephaly-like phenotype. Evidence from drosophila genetics has further established a genetic link between Cit-K and a protein Argonaut 1 (AGO1), which is required for proper functioning of the miRNA machinery (2). Experiments characterizing the role of miRNAs in the developing cortex demonstrate the requirement of miRNAs for differentiation of neural progenitor cells starting at embryonic day 12.5 (3). Together, this evidence links the role of miRNAs to neurogenesis and thus this relationship warrants further investigation. Here miRNA expression has been characterized between the wild type (wt) and the Cit-K mutant rat (Cit-$K^{fh/fh}$*).* Two bioinformatics approaches were utilized to analyze transcriptome analysis data comparing expression between the wt and Cit-$K^{fh/fh}$. Evaluation of miRNA expression between neural progenitor cells (NPCs) and cells grown in mitogen free media with BDNF+ (MFBCs) revealed diminished miRNA expression in Cit-$K^{fh/fh}$ NPCs upon removal of mitogens and addition of BDNF. Lastly, miRNA target prediction software was used to tabulate all highly predicted and verified gene targets for comparison with transcriptome analysis data. Gene targets of the down-regulated miRNAs in the MFBC population correlated with an up-regulation of those respective transcript levels in the transcriptome analysis dataset. These results confirm the possibility that miRNAs play a role in mediating the changes in transcript levels that appear upon the loss of Cit-K.

Introduction

Citron-Kinase (Cit-K$^{fh/fh}$) mutation results in a microcephaly like phenotype in rodents in which there is a substantial reduction in the size of the central nervous system, with little effect on the peripheral nervous system and most other organs (1). Although previous studies have suggested that Cit-K is predominantly required for the completion of mitosis and cytokinesis, such defects occur in only a fraction of the total population of cells suggesting that Cit-K's role may involve additional mechanisms (5). Unpublished data indicates that loss of the Cit-K gene function results in large scale differences relative to wild type in the level of thousands of transcripts, and this difference occurs prior to manifestations of defects in mitosis and cytokinesis (4). Molecular changes known to accompany changes in transcript levels include modifications to the chromatin state and changes in the activity of post-transcriptional regulatory molecules.

A major post-transcriptional regulatory mechanism is the miRNA system. Evidence from the study of the drosophila mutant *sticky* (a drosophila gene orthologous to Cit-K) has provided a link between Cit-K and miRNAs. Bosco et al. (2007) demonstrated the presence of a genetic interaction between Cit-K and AGO1, a key protein in the miRNA machinery. In the study by Bosco et al., an eye phenotype was compared between wild type and Cit-K deficient drosophila with and without over-expression of AGO1. Results showed the presence of a more severe rough-eye phenotype in Cit-K deficient drosophila upon over expression of AGO1, compared to a normal phenotype in the wild type. These observations suggest a hypothesis in which changes in processed miRNA levels that result from the loss of Cit-K contribute to the alterations in transcript levels in sticky/Cit-K mutants in drosophila and potentially in mammals as well.

In addition to the genetic link between Cit-K and the miRNA system in drosophila, additional evidence for a potential link comes from observations of the CNS phenotype of mouse knockouts of Dicer. Like AGO1, Dicer is a critical component of the miRNA effecter system. Experiments detailing the role of Dicer in the developing cortex reveal the necessity of miRNA processing beginning at embryonic day 12.5 for proper development of neurons (3). The Dicer knockout has a microcephaly phenotype that begins to appear at a similar time in development that microcephaly first emerges in the Cit-$K^{fh/fh}$. In addition, several studies have now shown the importance of individual miRNAs during development of the central nervous system (6, 7, 8, 9, 10, 11).

Review of the miRNA system

Over 1200 miRNAs have been detected in the human genome and recognition of their functional relevance to neuronal proliferation and differentiation is growing (6). miRNAs, ~22 nucleotides in their mature form, are endogenous small molecules that act to regulate gene expression at the post transcriptional level. Placement of miRNAs in the genome varies by location as well as prevalence. Three classes of miRNAs exist: exonic, intronic and intergenic. Their significance lies in their ability to broadly modulate gene expression through inhibition of translation or degradation of transcript in a partial complement fashion (6, 8, 10).

Biogenesis of miRNAs first occurs within the nucleus where they are transcribed as long primary-miRNAs that are poly-adenylated. Processing of this long transcript continues in both the nucleus and cytoplasm until formation of a mature 18-22 nucleotide miRNA. Regulation of miRNA functionality can occur starting at transcription, but also at each of the processing steps (12, 13, 14, 15). Processing begins in the nucleus where

Drosha cleaves the pri-miRNA into a hairpin loop referred to as pre-miRNA. Upon exportation into the cytoplasm through Exportin 5, the pre-miRNA undergoes cleavage by Dicer for formation of a double stranded intermediate. This double stranded molecule is then separated by the RNA-Induced Silencing Complex (RISC), by associating with one strand (guide strand) and displacing the other strand which is often degraded (passenger strand). The primary protein component of the RISC is AGO, a family of proteins comprised of 8 different subtypes (6). AGO is the catalytic component of the RISC and is characterized to two RNA binding domains: PAZ which binds the guide strand and PIWI that functions to cleave RNA (6, 10).

miRNAs function by guiding the RISC to the 3' UTR of an mRNA transcript. Association with RISC often induces instability in the mRNA through a variety of different mechanisms including: de-adenylation, blocking elongation, blocking translation, and 5' de-capping (16). Their broad regulatory ability arises from its ability to target genes through partial complementarity of only 7-8 base pairs between the miRNA and the 3' UTR of the mRNA (6, 8,10).

Prediction of miRNA targets

The recent availability of miRNA prediction software allows for the creation of models that demonstrate functional relationships between miRNAs and their gene targets. Initially, miRNAs were believed to only destabilize transcripts and not degrade them. Bartel et al. (2010) completed high throughout experiments to demonstrate that miRNAs predominantly result in degradation of large numbers of transcripts rather than just destabilization. One implication of this degradation is that data detailing the levels of individual transcripts can be compared with miRNA expression data to potentially

identify valid targets of particular miRNAs. Current miRNA target prediction software allows for prediction of thousands of gene targets that are scored based on probability of interaction between mRNA and miRNA. Predictions are tabulated based on algorithms that vary in method, but generally score feasibility of interaction based on complement of the miRNA seed sequence (nucleotides 2-7) to highly conserved regions on the 3' UTR of a gene (18). Target prediction results could be of great value for identification of miRNA targeted genes that show differential expression in the Cit-K$^{fh/fh}$. Specifically, comparison of changes in miRNA expression with changes in transcript level allows for identification of genes involved in mediating defects observed in Cit-K$^{fh/fh}$.

Summary of Thesis

In this thesis I sought to characterize miRNA expression in the Cit-K$^{fh/fh}$ mutant rat through a three step process including bioinformatics for miRNA expression profiling, qRT-PCR for validation of miRNA expression and cell population identification, and the use of prediction software for miRNA target prediction. A previously completed RNA-Seq comparison identified changes in transcript levels between WT and Cit-K$^{fh/fh}$. Investigation of these changes was accomplished using the Genome Analyzer-II by *Illumina* for parallel sequencing of total RNA that was converted into cDNA using Oligio-dT primers. Thus the data collected from this experiment consisted of all poly-adenylated transcripts which should include primary-miRNAs. Bioinformatics analysis of this same dataset allowed for characterization of miRNA expression in the Cit-K$^{fh/fh}$. Two bioinformatics analyses were conducted to identify the miRNAs that were expressed in the forebrain beginning at E11. The analyses provided knowledge of potentially expressed miRNAs and miRNA that were differentially expressed. More specifically, the

miRNAs that were chosen for further analysis were based on level of transcripts detected as well as level of differential expression and include: rno-mir-207, rno-mir-370, and rno-mir-466b. Rno-mir-22 was chosen through alternative means. These initial screens allowed for further investigations to identify the cells responsible for the changes in transcript levels. For this, a cell culture model was developed in which miRNA expression is compared between WT and Cit-K$^{fh/fh}$ in both neural progenitor cells and cells that are deprived of mitogens and exposed to BDNF in an attempt to mimic initial steps in the transition from mitotic precursor to differentiating neuron. miRNA expression between proliferating neural progenitor cells (NPCs) and mitogen free/BDNF+ cells (MFBCs) provide evidence for a decrease in miRNA expression upon removal of mitogens and addition of BDNF in Cit-K deficient NPCs. Lastly, miRNA prediction software was utilized in conjunction with RNA-Seq data from the Cit-K$^{fh/fh}$ to correlate differential miRNA expression and mRNA levels of predicted targets. miRNA target prediction software revealed that 51% of the predicted miRNA gene targets were up-regulated in the transcriptome analysis of the Cit-K$^{fh/fh}$. In conclusion, the data compiled in this thesis suggests that miRNAs may play a role in mediating some of the mRNA changes associated with the loss of Cit-K in maturing neural progenitor cells.

Results

Bioinformatics Analyses

Previous analysis of RNA-Seq data comparing transcript levels between WT and Cit-K$^{fh/fh}$ detailed differences in mRNA expression without providing any information on miRNA expression. The two bioinformatics analyses completed here intended to characterize miRNA expression in the Cit-K$^{fh/fh}$. Analysis I hinted at differential miRNA expression and allowed for selection of the miRNAs that were investigated here. However, it was later deemed faulty due to the methodology used for miRNA detection. See Sup. Fig. 1 for results of Analysis I and further explanation. Advancements in bioinformatics software, such as SeqMonk, allowed for visualization of all detected reads mapped out to their respective genomic locations. The bioinformatics analysis completed using SeqMonk resulted in detection (Fig. 1A) of 65 primary-miRNAs, of which 47 were predicted and 18 have been experimentally verified in rat. miRNAs were denoted as expressed if their associated genomic location showed >10 total reads between replicates(N=3) of either WT or Cit-K$^{fh/fh}$ from the RNA-Seq dataset. Detection included miRNAs that are found in exonic, intergenic, and intronic regions. In this analysis, a dataset less stringently aligned to the rattus genome was quantitated for maximal detection. Less stringently is defined as allowing reads to be aligned to specific portions of the genome when either completely homologous, with one mismatch, or two mismatches. Results indicate (Fig. 1B) expression of 5 exonic, 5 intronic, and 8 intergenic miRNAs that have been validated in rattus. Of the predicted miRNAs, there are 21 exonic, 7 intronic, and 19 intergenic. The majority of the detected miRNAs detected in this analysis are predicted miRNAs.

Of these detected miRNAs, there were 33 up-regulated miRNAs and 32 down regulated miRNAs. Results indicate an average fold expression (Fig. 1C) of 1.74 and 3.25 for up-regulated validated miRNAs and predicted miRNAs respectively. Average fold regulation of down regulated miRNAs slightly varied with -1.49 for validated and -1.99 for predicted miRNAs. Predicted miRNAs appears to be more differentially expressed for both up and down regulated miRNAs. Predicted miRNAs in Analysis II are based on predictions made by algorithms in ENSEMBL. This algorithm relies on two major factors: high homology of nucleotide sequences in rattus to conserved miRNAs and presence of secondary structure as verified by RNAFold. Analysis II confirmed the possibility that differential miRNA expression does exist in the Cit-K$^{fh/fh}$ mutant and additionally suggests that there is potentially a large number of developmentally relevant miRNAs in rattus which have yet to be experimentally validated. Interestingly, it is also apparent that, of the differentially expressed miRNAs, the up-regulated category is predominant. These results compelled us to further investigate miRNA expression in the Cit-K$^{fh/fh}$ in hopes of delineating their role in the manifestation of the changes in transcript levels that accompany the Cit-K$^{fh/fh}$ mutation.

Figure 1

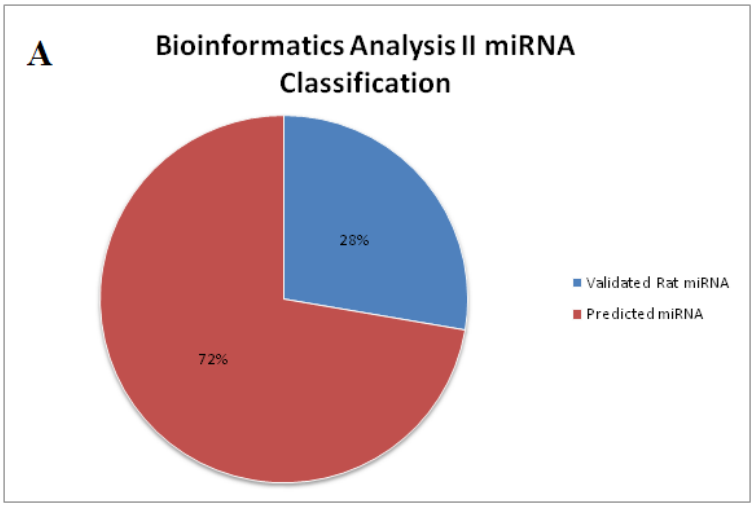
A
Bioinformatics Analysis II miRNA Classification
28%
72%
Validated Rat miRNA
Predicted miRNA

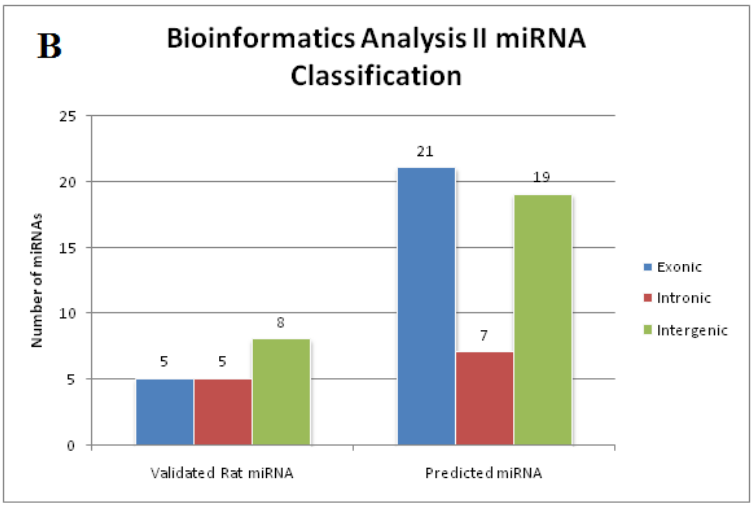
B
Bioinformatics Analysis II miRNA Classification
Number of miRNAs
25
20
15
10
5
0
5
5
8
21
7
19
Validated Rat miRNA
Predicted miRNA
Exonic
Intronic
Intergenic

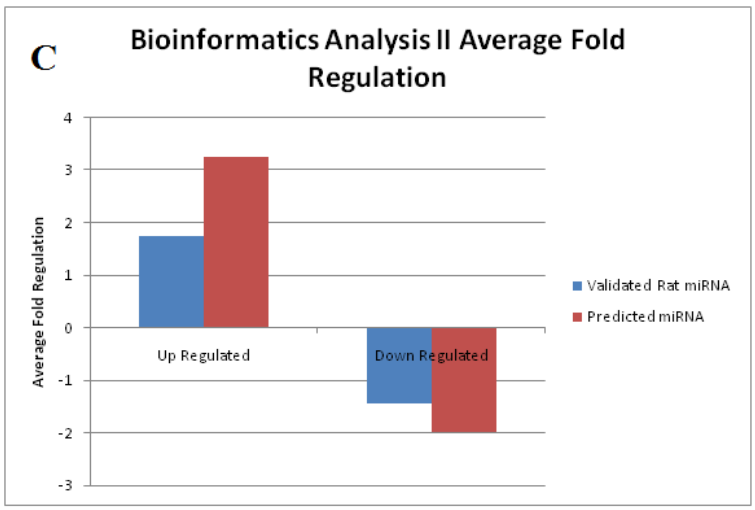
C
Bioinformatics Analysis II Average Fold Regulation
Average Fold Regulation
4
3
2
1
0
-1
-2
-3
Up Regulated
Down Regulated
Validated Rat miRNA
Predicted miRNA

Figure 1. Bioinformatics Analysis of Cit-K$^{fh/fh}$ RNA-Seq Dataset.

Analysis II relied on the use of SeqMonk for analysis. Detection of miRNAs here consists of quantitating the number of reads that corresponds to the genomic location of an annotated miRNA. N=3.

A) The pie chart illustrates the percentage of detected miRNAs that are either validated in rat or are predicted based on other species. Analysis II detected a total of 65 miRNAs with greater than 10 reads between the replicates of either WT or Cit-K$^{fh/fh}$.

B) A bar graph characterizing the types of miRNAs detected reveals detection of exonic, intronic, and intergenic miRNAs, with exonic and intergenic being the predominant transcript.

C) A bar graph revealing the average fold regulation of validated rat miRNAs and predicted miRNAs suggest a predominant up-regulation of miRNAs in the Cit-K$^{fh/fh}$. Average fold regulation is separated between up-regulated and down-regulated miRNAs. Average fold regulation is the average of the ratios of $2^{\square\square CT}$ between WT and Cit-K$^{fh/fh}$ for all miRNAs in that specific category.

Evaluation of miRNA expression in the Cit-K$^{fh/fh}$ mutant

Upon identification of miRNAs that were shown to be differentially expressed in the RNA-Seq data analysis, confirmation of their expression was completed using Quantitative Real Time PCR. The miRNAs that were initially evaluated include: rno-mir-466b, rno-mir-370, and rno-mir-207. Expression analysis of these miRNAs was conducted on both E11 forebrain lysate and on E11 neural progenitor cells. Results from E11 forebrain lysate indicate (Fig. 2A, B) down regulation of all evaluated miRNAs. Expression analysis (Fig. 2C, D) of Passage 3, E11 NPCs paralleled differential expression of rno-mir-466b and rno-mir-370 but not rno-mir-207. The differential miRNA transcript levels appear to be potentiated in the passage 3 NPCs, specifically rno-mir-370 which is almost 8 fold down regulated in comparison to the 2 fold down regulation observed in the E11 forebrain. These results demanded identification of the cells responsible for the differences in miRNA transcript levels.

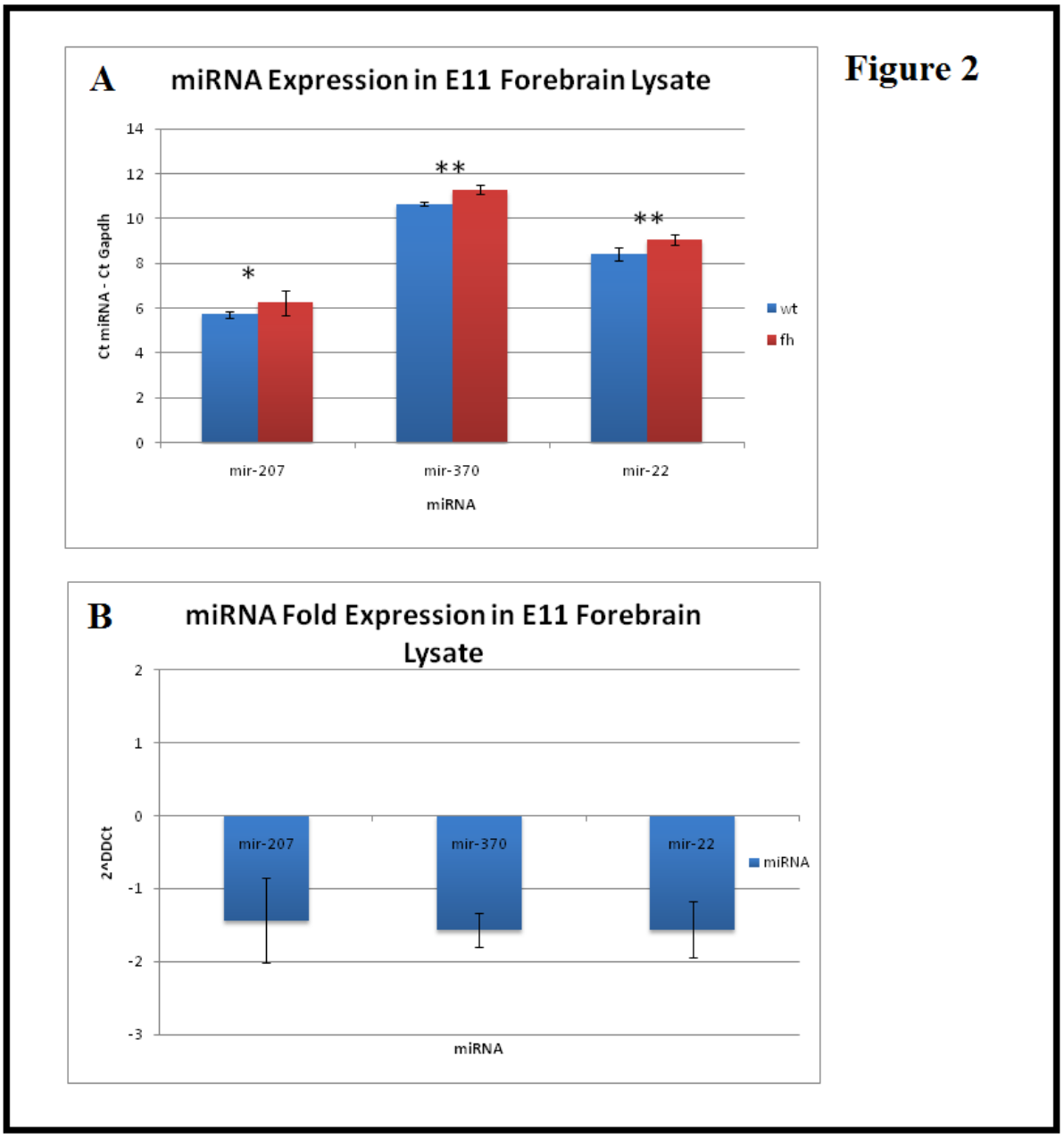

Figure 2. miRNA expression comparison between wild type and Cit-K$^{fh/fh}$ rats.

A) Quantitative RT-PCR results showing miRNA expression in Cit-K$^{fh/fh}$ E13 forebrain lysate relative to wild type. Data represents WT and Cit-K$^{fh/fh}$ Ct values that have been normalized to Gapdh. N=2 in triplicates.

B) Fold expression of select miRNAs using $2^{\square\square Ct}$ suggests down regulation of select miRNAs in Cit-K$^{fh/fh}$ relative to WT. Comparison of WT to Cit-K$^{fh/fh}$. N=2 in triplicates.

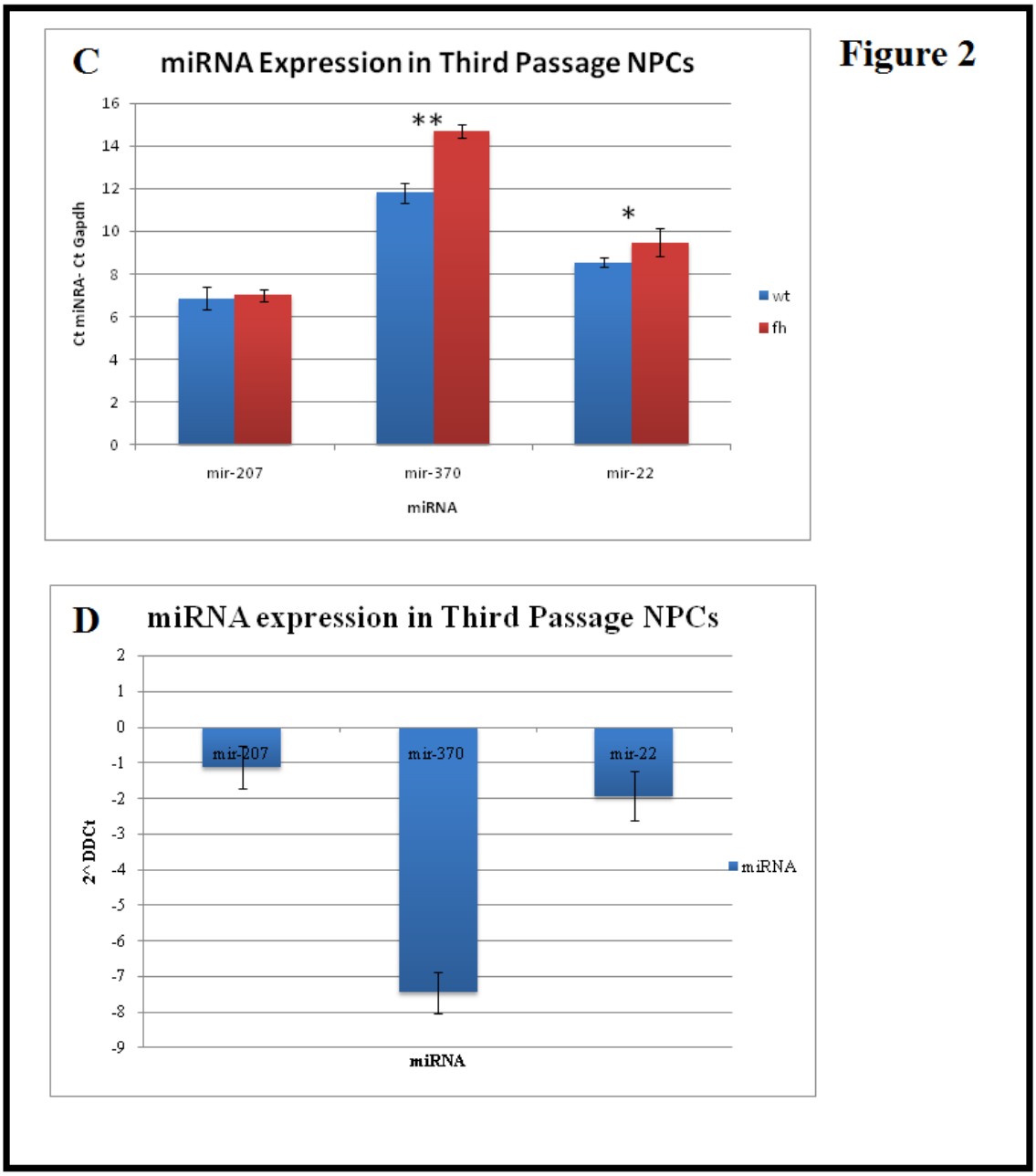

Figure 2

Figure 2. miRNA expression comparison between wild type and Cit-K$^{fh/fh}$ rats.

C) Quantitative RT-PCR results showing miRNA expression in Cit-K$^{fh/fh}$ E11 Passage 3 cultured NPCs relative to wild type. Data represents WT and Cit-K$^{fh/fh}$ Ct values that have been normalized to Gapdh. N=2 in triplicates.

D) Fold expression of select miRNAs using $2^{\Delta\Delta Ct}$ also suggests down regulation of select miRNAs in Cit-K$^{fh/fh}$ relative to WT. Comparison of WT to Cit-K$^{fh/fh}$. N=2 in triplicates.

** P< .0001 (Student's t-test; 1 tailed) compared with WT.

*P< .05 (Student's t-test; 1 tailed) compared with WT.

Error bars indicate Standard Deviation.

miRNA Expression in a in vitro model to mimic the onset of differentiation

miRNA expression analysis (Fig. 3 A) between WT and Cit-K$^{fh/fh}$ E11 NPCs showed mostly minimal differences in miRNA expression of rno-mir-466b, rno-mir-370, rno-mir-207, and rno-mir-22. These results differ from the expression analysis conducted on Passage 3 NPCs, which demonstrated differential expression, suggesting intrinsic expression differences in cells at different developmental time points. Previous studies may help explain differences in expression levels at these two time points. Research on intracellular development timers in astrocytes, oligodendrocytes, and ependymal cells demonstrates that the differentiation of these cells grown in culture generally parallels the timeline of differentiation in the brain (21). This data suggests that these cells contain an intrinsic counting mechanism that signals differentiation rather than solely extrinsic signals (21). Although their results did not conclusively provide any evidence that neurons too rely heavily on intracellular timers, it may be possible that they do to some extent (31). Due to differences in cell cycle for cells from passage 1 and passage 3, it is possible that the differences in miRNA transcript levels detected could be attributed to the fact that these cells are at different time points in their developmental timeline and thus have different expression patterns. This provides reason to believe that the differences in transcript levels observed in the expression analyses of miRNAs may actually be a result of the differing developmental stage of the cells isolated. Attributing miRNA expression differences between E11 forebrain and E11 NPCs to varying cell populations in the forebrain is plausible and requires further experimentation. Identification of the cells most reliant on miRNA expression would provide insight on the role of these variably expressed miRNAs.

De Pietri Tonelli et al. suggests that miRNAs are crucial for the differentiating population of cells, as demonstrated by massive reductions in neuronal layers in mutants that lack crucial miRNA machinery(3). This evidence provided reason to assess miRNA expression in cells at a later developmental time point. To identify the cell population responsible for the differential miRNA transcript levels detected in our initial expression analyses and assess miRNA transcript levels in cells at a later developmental stage, a cell culture model was developed to mimic the onset of cellular differentiation. Results from Li et al. (2009) showed that exposure of 40 ng BDNF / 1ml media to NPCs induced differentiation and elongation into neurites as demonstrated by TUJ1+ staining. Additional evidence also suggests that BDNF potentiates differentiation of NPCs (19, 20). Based on this information, a model (Sup. Fig.3) was developed for comparison of miRNA expression between NPCs that were grown in proliferative media (egf and bFGF) and NPCs that were inducted towards a path of differentiation via removal of the proliferative media and addition of BDNF (MFBCs).

miRNA expression of rno-mir-466b, rno-mir-370, rno-mir-22 and rno-mir-207 were evaluated in this in-vitro model in order to confirm this hypothesis. Results (Fig. 3C,D) comparing miRNA expression between proliferating wild type NPCs and wild type MFBCs demonstrate an up-regulation of all miRNAs investigated. In concert with results from De Pietri Tonelli et al. (2008), our results demonstrate an increased need for miRNAs during induction towards differentiation as indicated by the increase in miRNA expression at that time. However, in contrast, results (Fig. 3B) comparing expression between proliferating Cit-K$^{fh/fh}$ NPCs and Cit-K$^{fh/fh}$ MFBCs did not demonstrate significant differences in miRNA expression. Our data suggests that loss of Cit-K

disrupts the miRNA system early on, possibly during proliferation, thus resulting in the detected deficiency in miRNA expression upon maturation of neural progenitor cells. Expression analysis (Fig. 3E,F) between wild type MFBCs and Cit-K$^{fh/fh}$ MFBCs further demonstrates the effects of the loss of Cit-K on miRNA expression. All four miRNAs investigated show a significant down regulation in Cit-K$^{fh/fh}$ MFBCs, with rno-mir-466b showing an almost 3.5 fold down regulation. Figure 4 concludes and well illustrates the transcript level differences in the two cell types: NPCs and MFBCs. It is clear here that, in the MFBCs, the magnitude of fold expression in the Cit-K$^{fh/fh}$ is greatly potentiated relative to the differences observed in the NPCs. The proliferating NPCs demonstrate minimal differences in miRNA expression in the Cit-K$^{fh/fh}$ relative to WT, but it is clear that a significant reduction in miRNA expression appears upon onset of differentiation, based on our model.

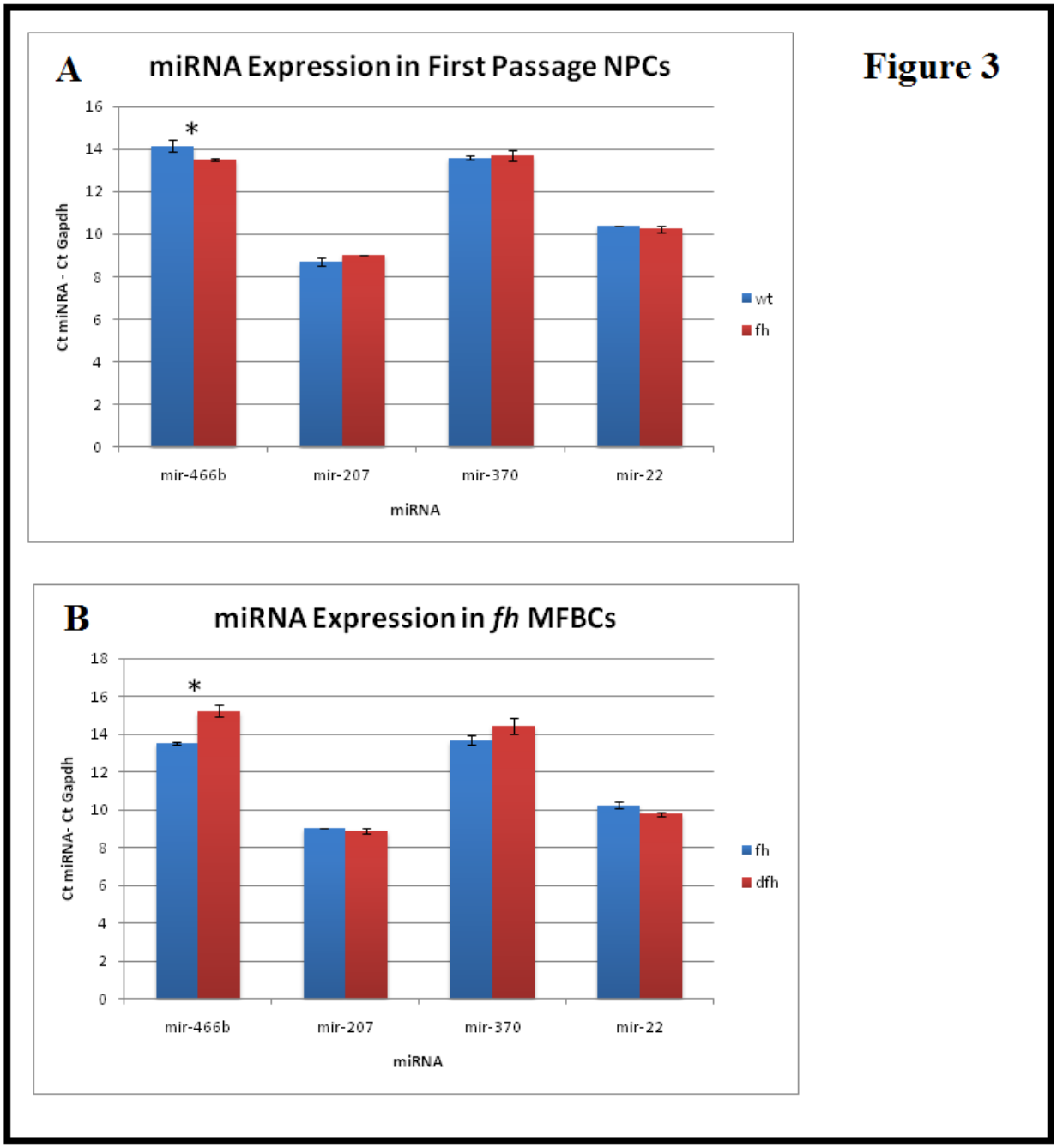

Figure 3

Figure 3. miRNA expression in Passage 1 NPCs in a mitogen deprivation/BDNF addition experiment

A) E11 cultured NPCs mostly display no differential miRNA expression. Data represents WT and Cit-K$^{fh/fh}$ Ct values that have been normalized to Gapdh. N=3.

B) E11 Cit-K$^{fh/fh}$ cultured NPCs display minimal change in expression upon addition of BDNF and removal of EGF and bFGF. Data represents Cit-K$^{fh/fh}$ NPCs and Cit-K$^{fh/fh}$ MFBCs Ct values that have been normalized to Gapdh. N=3.

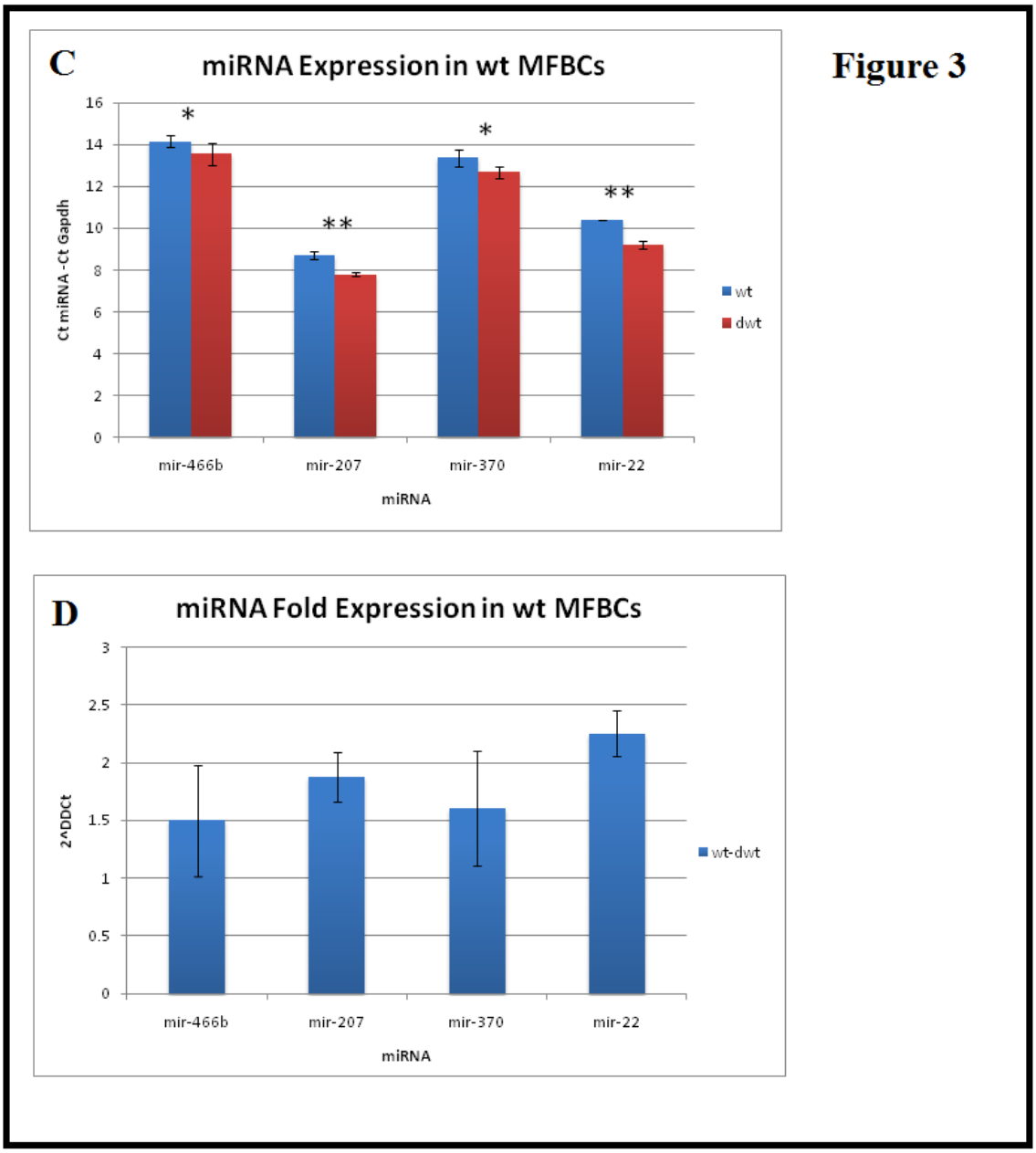

Figure 3

Figure 3. miRNA expression in Passage 1 NPCs in a mitogen deprivation/BDNF addition experiment

C) E11 WT cultured NPCs display increased miRNA expression upon addition of BDNF and removal of EGF and bFGF. Data represents WT NPCs and WT MFBCs Ct values that have been normalized to Gapdh. N=3.

D) Fold expression determined using $2^{-\Delta\Delta Ct}$. Comparison of WT NPCs and WT MFBCs. N=3. A significant up-regulation of all miRNAs investigated appears in NPCs upon removal of mitogens and addition of BDNF.

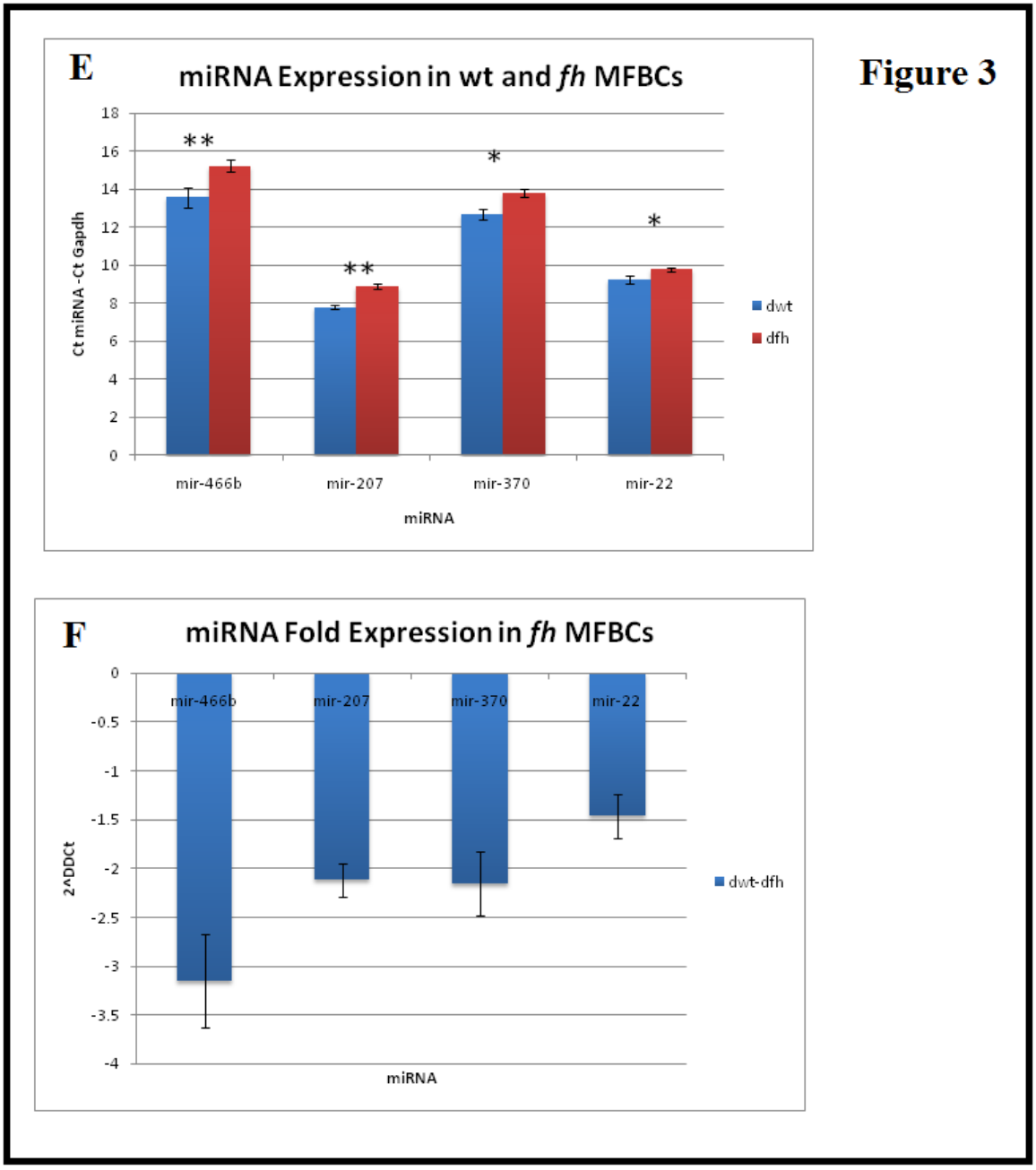

Figure 3

Figure 3. miRNA expression in Passage 1 NPCs in a mitogen deprivation/BDNF addition experiment

E) E11 MFBCs display significant decrease in miRNA expression. Data represents WT MFBC and Cit-K$^{fh/fh}$ MFBC Ct values that have been normalized to Gapdh. N=3.

F) Fold expression determined using $2^{\Delta\Delta Ct}$. Comparison of WT MFBC and Cit-K$^{fh/fh}$ MFBC. N=3. A significant decrease in miRNA expression appears in Citron-k deficient NPCs upon removal of mitogens and BDNF addition.

** P< .0001 (Student's t-test; 1 tailed)

*P< .05 (Student's t-test; 1 tailed)

Error bars indicate Standard Deviation.

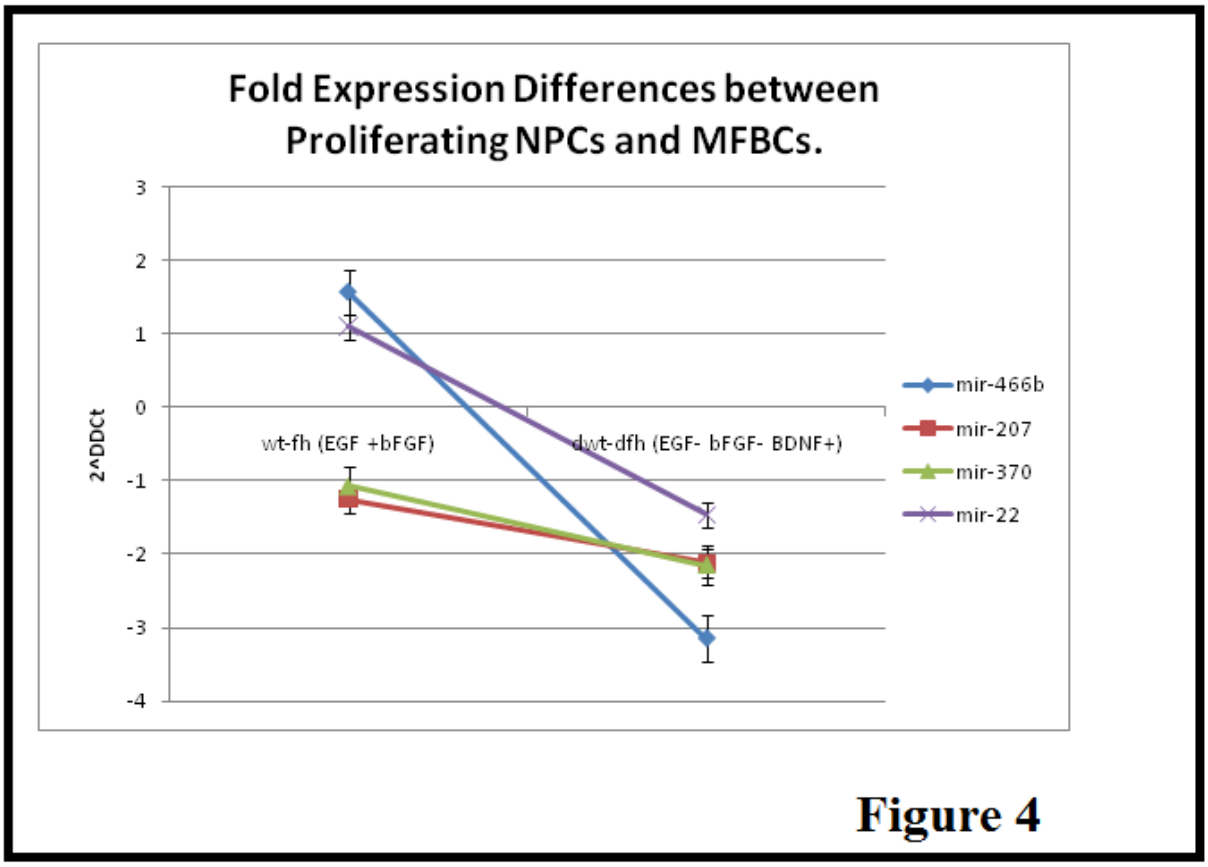

Figure 4. miRNA expression deficits in MFBCs.
A graphical representation demonstrating an overall decrease in miRNA expression in MFBCs compared to NPCs between wild type and Cit-K$^{fh/fh}$. Fold expression determined using $2^{\square\square Ct}$ comparing wild type to Cit-K$^{fh/fh}$. N=3. Error bars indicate Standard Deviation.

miRNA Target Prediction

miRNA target prediction has become easily accessible due to online software that have the ability to compile all verified miRNA targets and predicted miRNA targets based on algorithms (23). These prediction algorithms have led to successful identification of miRNA targets in many experiments (7). Successful identification of targets for rno-mir-466b, rno-mir-370, rno-mir-22 and rno-mir-207 will allow for elucidation of the role these miRNAs play in mediating the transcriptional changes associated with the Cit-K$^{fh/fh}$. Target identification here consisted of combining target prediction and RNA-Seq data for a more educated prediction of targets. Using miRWALK for target prediction, a total of 152 targets were identified for the four miRNAs investigated. Targets were only denoted as predicted if they were predicted by three different algorithms and were expressed in the RNA-Seq dataset. Although it is known that miRNAs have the ability to interact with thousands of targets, it is important here to identify targets that show significance to the transcriptional changes observed in the Cit-K$^{fh/fh}$ mutant. Once tabulated, the targets' expression was identified using the RNA-Seq data. Transcriptional changes in the Cit-K$^{fh/fh}$ (Fig. 5A) show that 23.7% of the transcripts are up regulated and 13.8% are down regulated. Results show (Fig. 5B) that of the 154 predicted targets identified, 51% are up-regulated and 28% are down-regulated based on the threshold for up/down regulation set at 1.l and -1.1 fold expression. In addition, further analyses (Sup. Fig 5), in which the threshold for up regulation was made more stringent from 1.1 to 1.3 and 1.5, were conducted to assess the strength of the relationship between miRNA down regulation and mRNA up regulation. Analysis shows

that even after changing the threshold form 1.1 to 1.3, 26% of the 154 predicted targets are still up regulated. The value declines to 15% when the cut off is made to 1.5 fold expression. The small changes in transcript levels observed due to differential miRNA levels is in concert with the method by which miRNAs function to regulate gene expression. miRNAs have been shown to broadly modulate gene expression of thousands of transcripts, and thus it would make sense that the small changes in fold expression of these transcripts observed in the Cit-$K^{fh/fh}$ could be attributed to differential miRNA transcript levels rather than other stronger regulators of expression. These results further strengthen the link between the decrease in miRNA expression in the MFBCs in the Cit-$K^{fh/fh}$ and the up-regulation in transcript levels observed in the Cit-$K^{fh/fh}$.

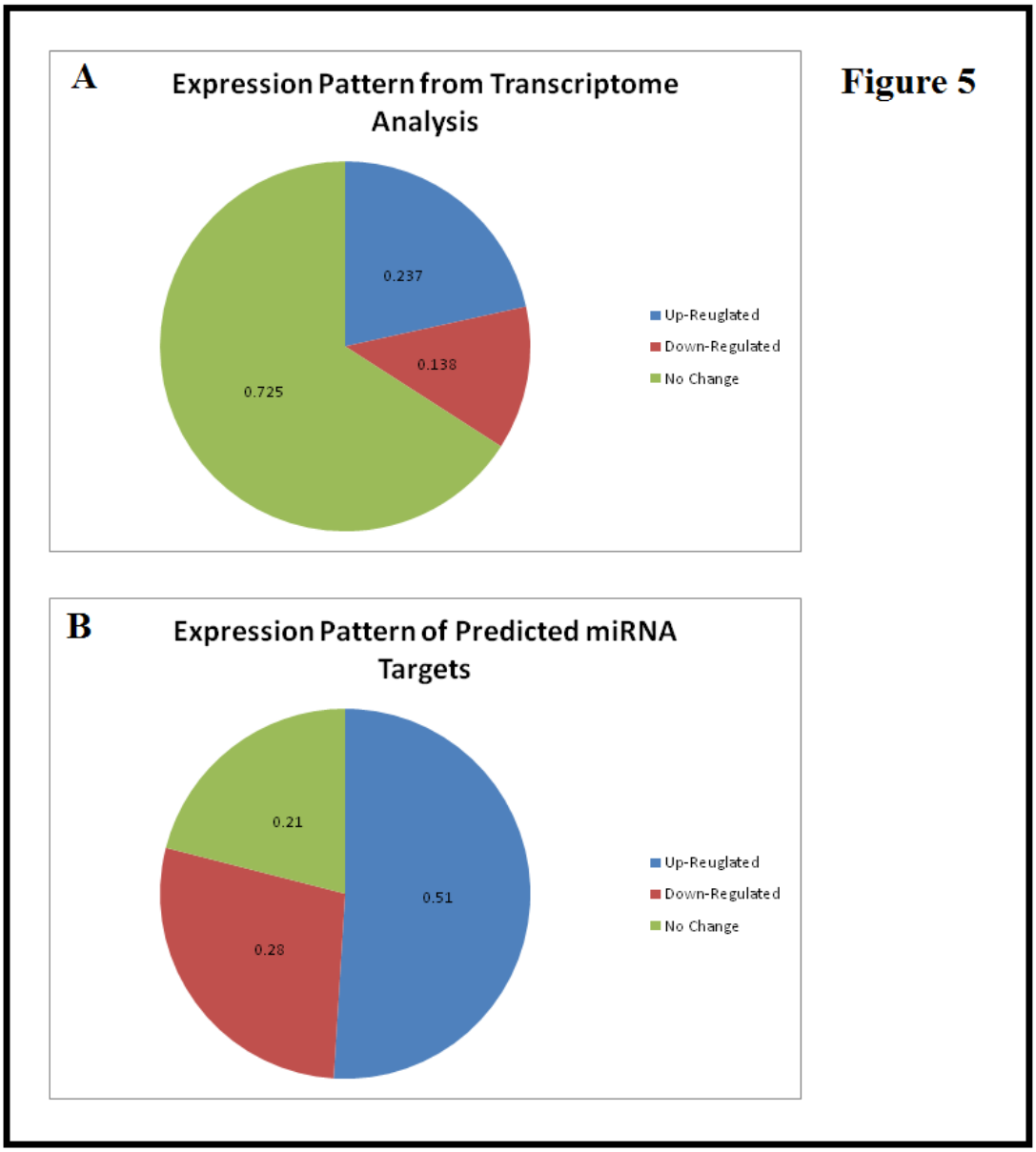

Figure 5

Figure 5. miRNA Target Prediction

A) Pattern of gene expression for all detected transcripts in the deep sequencing dataset between WT and Cit-K$^{fh/fh}$.

B) Pattern of gene expression in deep sequencing dataset for all verified miRNA targets in addition to predicted miRNA targets that were predicted by three separate algorithms. Total of 154 targets assessed of the 4 investigated miRNAs (rno-mir: 370, 207, 22, 466b).

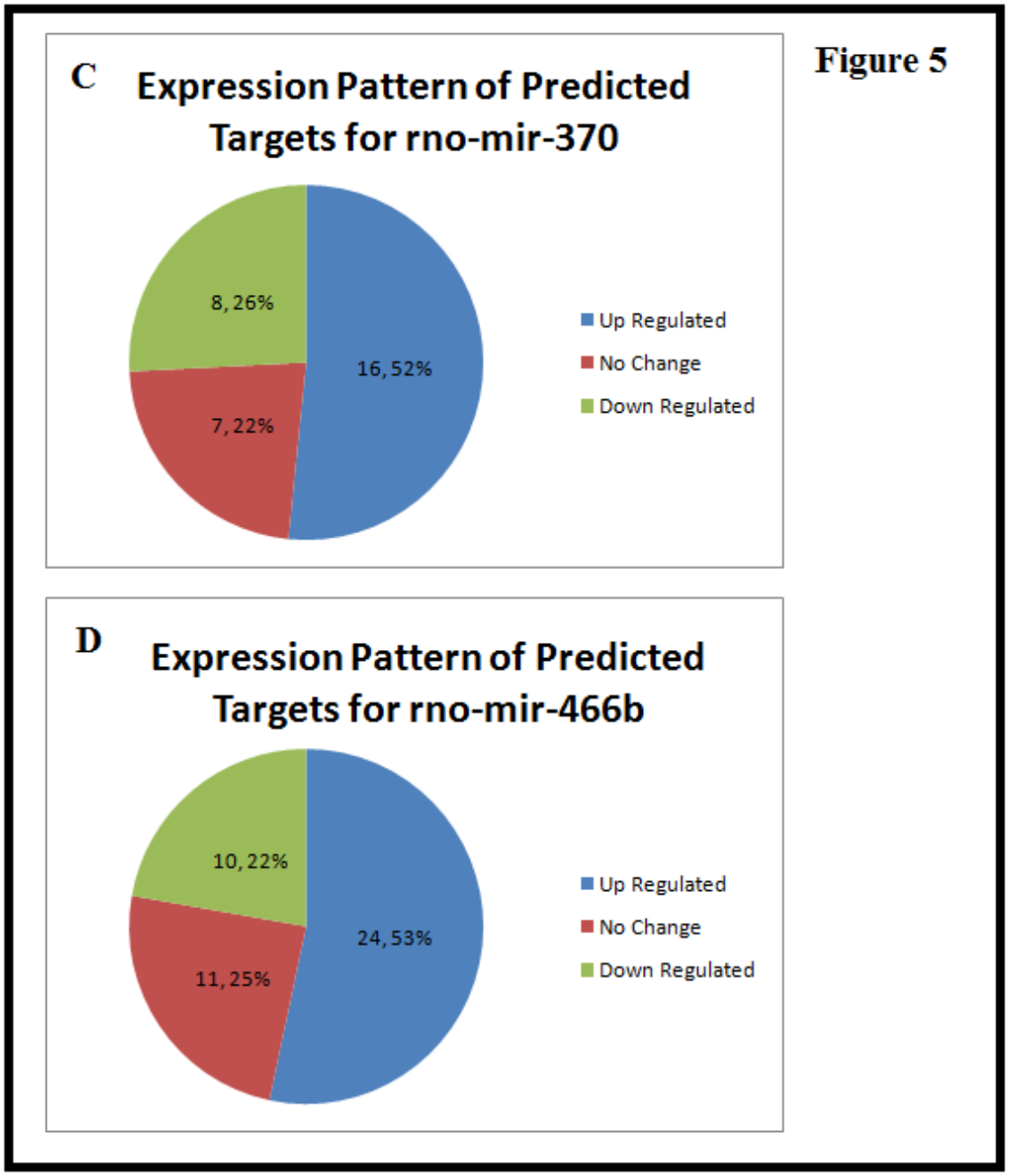

Figure 5

Figure 5. miRNA Target Prediction

C) Pattern of gene expression in RNA-Seq dataset of all known and predicted targets assessed for rno-mir-370 demonstrate a 52% up-regulation of its predicted targets.

D) Pattern of gene expression in RNA-Seq dataset of all predicted targets assessed for rno-mir-466b demonstrate a 53% up-regulation of its predicted targets.

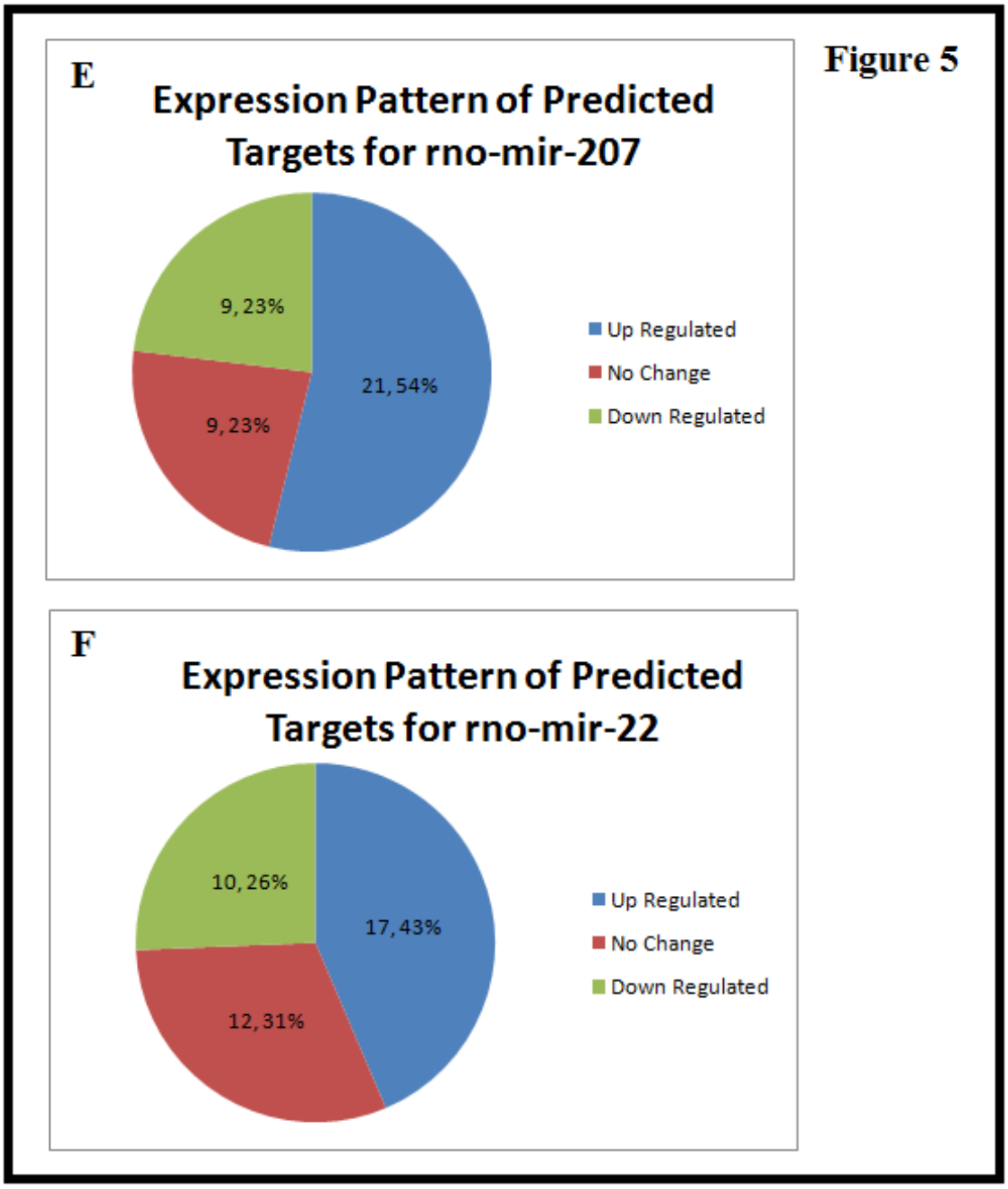

Figure 5. miRNA Target Prediction

E) Pattern of gene expression in RNA-Seq dataset of all predicted targets assessed for rno-mir-207 demonstrate a 54% up-regulation of its predicted targets.

F) Pattern of gene expression in RNA-Seq dataset of all known and predicted targets assessed for rno-mir-22 demonstrate a 43% up-regulation of its predicted targets.

Discussion

Together, these findings begin to characterize miRNA expression in the Cit-K$^{fh/fh}$ and further strengthen the link between Cit-K and the miRNA machinery. In addition to the genetic interaction known to exist between AGO1 and Cit-K, these new findings verify that Cit-K does play a role in modulating miRNA expression at the transcriptional level as demonstrated by differences in primary-miRNA transcripts present. Initial bioinformatics analysis of the RNA-Seq dataset provides evidence for differential expression of primary-miRNAs as a result of the loss of functional Cit-K expression. qRT-PCR further validates these findings and clearly demonstrates differential primary-miRNA expression in E11forebrain lysate and third passage NPCs. Expression analyses of miRNAs in E11 first passage NPCs demonstrate minimal differences in expression and are in sync with the notion that expression patterns change intrinsically in a timely fashion that parallels development when grown in culture. Exaggerated down regulation of miRNA expression is apparent in the Cit-K$^{fh/fh}$ MFBC population relative to the differences observed in the NPCs. The lack of significant differences in miRNA expression observed between the Cit-K$^{fh/fh}$ NPCs and Cit-K$^{fh/fh}$ MFBCs suggests that Cit-K is required for the proper function of the miRNA machinery prior to the onset of differentiation. The large differences in miRNA expression observed in the MFBC population can possibly be attributed to the disruption in the miRNA machinery before the onset of differentiation that inflates the disparity in expression once progenitors begin to differentiate. Based on the results of this thesis, I conclude that Cit-K has a possible role in the initiation of miRNA expression patterns required for regulating gene expression during the onset of cellular differentiation.

Successful identification of targets of these down regulated miRNAs in the Cit-K$^{fh/fh}$ could potentially allow for identification of target pathways that could alleviate the microcephaly phenotype observed. Finding such interactions would allow for characterization of important miRNA-gene interactions that are vital for facilitating transitions between proliferation and differentiation. Recent evidence provides a model for the epigenetic regulation of a specific miRNA that has been shown to modulate the balance between proliferation and differentiation. Zhao et al. (2010) identified a link between mir-184 and Numbl, a pathway that results in disruption of the balance between proliferation and differentiation when perturbed. In addition, the expression of that miRNA is epigenetically regulated. Changes in expression of MDB1, a protein involved in epigenetic gene silencing, can result in significant changes in expression of mir-184. This complex regulatory network has been shown to regulate cellular transition from proliferation to differentiation. Multiple miRNA-target gene interactions like these have been identified in modulating cell fate and offer promise for further investigation of miRNAs in the Cit-K$^{fh/fh}$ mutant. Similarly, the transcriptional changes associated with the Cit-K$^{fh/fh}$ mutant are largely a result of epigenetic changes (4). It is possible that miRNA –gene target interactions similar to that seen with mir-184 exist in the Cit-K$^{fh/fh}$.

Future studies will undoubtedly be directed towards identification of miRNA-gene target interactions. Two major findings have emerged from network analysis of all predicted up-regulated genes. The first finding involves the identification of a gene network with a high degree of convergence onto a gene SMAD3 (Sup. Fig. 5), which is a signaling substrate for the transforming growth factor β/activin signaling pathway (24). The second finding is the ubiquitous targeting of a gene in that network, Nr3c1, by rno-

mir-22, rno-mir-207, and rno-mir-466b. Changes in stringency for the threshold of up regulation to 1.5 still results in a network that modulates Nr3c1, thus further strengthening the possibility of this relationship between these 3 down regulated miRNAs and their predicted target genes. The majority of the gene interactions in the SMAD3 network are composed of target genes that are only slightly differentially expressed, and thus the network collapses if genes that are only up regulated more than 1.5 are used.

The network is composed of direct interactions with Smad3 by: NR3C1, ZEB1, PPP2R2D, PTN, and MECOM. In addition, FOSL1, MAF, and NR3C1 all interact with Jun, which in turns regulates Smad3 activity. Many of these genes appear to interact with SMAD3 in a push- pull fashion such that NR3C1, MECOM, PP2RD2, and PTN repress SMAD3 activity, and ZEB1 potentiate its activity (24, 25, 26, 29, 30). Coincidently, it appears that the majority of the up-regulated predicted targets act to repress SMAD3 activity and thus suggest a negative impact on differentiation. The majority of the genes in this network have also been characterized to individually have an impact on differentiation when perturbed (22, 26, 27, 28). Direct evidence that SMAD3 dependent differentiation exists in the nervous system is indicated by results that show the requirement of SMAD3 activity for induction of neurogenic genes such as NeuroM and p27 for induction of differentiation (28). In addition, a model for chondrocyte differentiation implicates SMAD3 as being required for association with SOX9 and P300 for histone acetylation (27). Conserved function in the CNS of SMAD3 would implicate it in playing an epigenetic role in cell differentiation in the CNS as well.

This complex regulatory network shown to be important for the induction of differentiation may potentially be the target of down-regulated miRNAs in the Cit-$K^{fh/fh}$.

Loss of Cit-K gene function may potentially result in aberrant expression patterns for extremely important signaling pathways such as SMAD3. One mechanism by which this may occur is through the lack of post-transcriptional inhibition of these targets through miRNAs. The results of this thesis demonstrate a down regulation of miRNAs predicted to target genes that appear to converge on SMAD3. In addition, the majority of the up-regulated targets act to attenuate SMAD3 activity. These observations suggests that attenuation of the SMAD3 signaling pathway as may be present in the Cit-K$^{fh/fh}$ could potentially attribute to the massive reductions seen in the cortical layers as a result of diminished differentiation.

Educated predictions as these could lead to successful confirmation of miRNA targets that are involved in determining the developmental state of a cell. Although identifying direct relationships between miRNAs and target genes is informational, gaining a broader understanding of where Cit-K may interact with the miRNA system may be more beneficial to understanding the role of the miRNA system on the development of the CNS.

Our results have provided a framework for the identification of more miRNA-gene target interactions that may have important implications for mediating the balance between proliferation and differentiation. Elucidation of these targets may result in the discovery of new pathways that regulate cellular development and will provide insight for the advance of novel techniques for a more efficient manipulation of stem cells that can one day be applied therapeutically.

Methods

Bioinformatics Approach 1

Data gathered from deep sequencing using *Illumina* technology was utilized for both bioinformatics approaches. Expression analysis between WT and Cit-$K^{fh/fh}$ identified total changes in all poly- adenylated transcripts. Output data used for this analysis contained all 35 base pair reads that matched to only one (the best alignment) chromosomal position, commonly referred to as the ELAND s_N_Sorted. Alignment to the rattus norvegicus genome version 4 was completed using ELAND, a software package used with *Illumina* datasets. Filtration consisted of removing adapter sequences and removing reads without alignment. In addition, only non-exonic reads were analyzed. All aligned 35 base pair reads of non-exonic origin were then blasted against all experimentally known miRNAs that are listed on www.mirBase.com. Reads that demonstrated homology with a given mature miRNA (~18-22 nucleotides) were then annotated as that particular miRNA. Quantitation was conducted for an n=3 WT versus Cit-$K^{fh/fh}$. Replicates were normalized for total number of reads in that sample followed by averaging of normalized replicates. Ratios were then taken to compare WT versus Cit-$K^{fh/fh}$. Only miRNAs with a total of 10 reads per treatment, either WT of Cit-$K^{fh/fh}$, were further analyzed. The miRNAs with the highest level of expression and maximal difference in expression between treatments were then further analyzed.

Bioinformatics Approach 2

Analysis of deep sequencing data here consisted of the use of less stringently aligned reads. ElAND s_N_Export dataset consist of 35 base pair reads annotated to chromosomal positions dependent on exact match, 1 base pair error, and 2 base pair error.

SeqMonk, software compatible with ELAND aligned data, allows for visualization and analysis of where all reads fall along each chromosome. This software matches deep sequencing data to chromosomal positions that are fully annotated for miRNA genomic locations. Analysis for miRNA expression was conducted by comparing the number of mapable reads that corresponded to genomic locations for the hairpin sequence of a miRNA(70-140 basepairs). Quantitation was conducted for an n=3; WT versus Cit-$K^{fh/fh}$. Replicates were normalized for total number of reads followed by averaging of normalized counts for each treatment. Ratios were then taken to compare WT versus Cit-$K^{fh/fh}$. Only miRNAs with a total of 10 reads per treatment, either WT of Cit-$K^{fh/fh}$, were further analyzed. The miRNAs with the highest level of expression and maximal difference in expression between treatments were then further analyzed.

Tissue Extraction

Cit-K heterozygous pregnant rats with were anesthetized with isoflurane prior to cervical dislocation. Subjects were immediately dissected for E11 WT and Cit-$K^{fh/fh}$ embryos. Forebrain tissue was isolated and maintained in HBSS in addition to removal of tail clip for genotyping. Forebrain tissue was then homogenized and used for RNA isolation via TRIZOL kit, or cultured to enrich for neural progenitor population. Dissociated primary culture of E11 forebrain tissue is started with HBSS wash of tissue and dissociation with Trypsin-EDTA. Cells are then neutralized with Trypsin inhibitor and centrifuged at 1500 rpm for 8 min. Pellet is re-suspended in growth medium and platted for culture.

Cell Culture

All cells (both WT and Cit-$K^{fh/fh}$) were cultured in 6 well (Costar 3516) culture plates with nitric acid washed cover slips. Cover slips were coated with PDL (1:100 in HBSS)

and laminin (1:200 in HBSS). Mitogen+ growth media consisted of 97% DMEM, 1% PenStrept, 1% N2, 2% B27, .5% Sodium pyruvate, .5% L- Glutamine, .02% bFGF, and .002% EGF. Mitogen free BDNF+ media paralleled growth media however EGF and bFGF were substituted with 100 ng BDNF/1ml media. Termination of cell cycle and initiation of differentiation was induced using a step wise BDNF media change in which media would be changed in four steps. BDNF+ media was added in 25% increments per media change which occurred every 2 days. All cells were incubated at 37º C. For proliferating NPCs, cells were allowed to proliferate to 80-90% confluent at which point they were split (1:2) and allowed to proliferate to 80-90% confluent and harvested. The remaining plates began treatment after 3 days of proliferation with BDNF+ media as detailed above. MFBCs were harvested between 9-11 days after initial split. RNA was immediately isolated upon cell harvest.

RNA Isolation

RNA was isolated from an n = 3 of WT and *fh* E11 neural progenitor culture and n=2 forebrain tissue using the Ambion RNAqueous kit and TRIZOL respectively. NPCs were homogenized with the addition of 500 µL of 10 µg/mL Lysis/Binding solution. NPCs were sonicated followed by centrifugation for 2-3 minutes at 16000xg for purification. Subsequently, 500 µL of 64% Ethanol was pipetted into each lysate and vacuum filtered through a filter cartilage. Lysates were centrifuged and any flow-through was discarded. Filter cartridges were then washed with 700 µl of Wash Solution #1 and two 500 µl aliquots of Wash Solution #2/3. Flow-through was discarded after each wash, and the resulting samples were centrifuged for 3 minutes in order to remove any excess wash solution. After transferring to a fresh collection tube, bound RNA was eluted twice using

preheated (80º C) Elution Solution. A 30-second centrifugation after each aliquot was performed to collect the eluate. Forebrain tissue was homogenized in 1ml TRIZOL reagent per 50-100mg tissue. Homogenized samples are then incubated for 15 min at 30º C. Chloroform (.2 ml / 1 ml TRIZOL) is added and hand shaken for 15 seconds followed by incubation for 3 minutes at 30º C. Samples are centrifuged and at 12000g for 10 minutes resulting in phase separation. The aqueous phase is isolated and RNA is precipitated upon addition of isopropyl alcohol (.5 ml/ 1 ml TRIZOL reagent used). Sample is incubated for 10 minutes at 30º C at 12000g. RNA pellet visibility emerges upon washing of the RNA pellet with 75% ethanol (1 ml ETOH/1ml TRIZOL). Sample is vortexed followed by centrifugation for 5 minutes at 7500g. Mixture is air dryed followed by re-suspension in RNase-free water. RNA concentrations were measured for each sample using the Nanodrop© spectrophotometer at 260 nanometers. Isolated RNA was stored at -20º C.

cDNA Synthesis

cDNA synthesis was conducted using Invitrogen SuperScript III. Briefly, 1 µg of isolated RNA from each sample (n = 3 forebrain RNA or n = 3 neural progenitor culture RNA) was pipetted into a tube containing 1 µl 50 µM oligo$(dT)_{20}$ primer. Another 1 µl of 10 mM dNTP mix was added, and the total volume was brought up to 10 µl using DEPC-treated water. After 5 minutes of incubation at 65º C and 1 minute on ice, 10 µl cDNA Synthesis Mix was added to each tube. Synthesis Mix contained 2 µl 10X RT buffer, 4 µl 25 mM $MgCl_2$, 2 µl 0.1M DTT, 1 µl RNaseOUT and 1 µl SuperScript III RT. Following centrifugation, the mixtures were incubated for 50 minutes at 50º C, and then for 5 minutes at 85º C to terminate the reaction. Samples were centrifuged and 1 µl RNase H

was pipetted into each tube to remove any RNA. After a final incubation of 20 minutes at 37º C, synthesized cDNA was stored at -20º C.

Primer Design for miRNAs

Primers required for qRT-PCR completion were designed using the Primer3 software (http://frodo.wi.mit.edu/primer3). miRNA hairpin loop sequences used for primer design were selected from the miRBase (http://www.mirbase.org). Primers were designed with specific parameters for proper function. The product size range was restricted to between 105 and 175 base pairs for optimal qRT-PCR amplification. Primer GC percentage was kept within a range of 20 to 80 and a GC clamp was added to promote stronger binding affinity. Primer T_m was optimized at 65º C; with a 60º C to 70º C range, and primer size was limited to 18-22 base pairs. Resulting primers from Primer3 were assessed for specificity using NCBI Blast (http://blast.ncbi.nlm.nih.gov/Blast.cgi).

Quantitative RT-PCR

QRT-PCR was performed using the Applied Biosystems ABI 7500 Fast Real Time PCR System. Plates were prepared with reaction volumes of 20 µL per well including the following: 9 µL primer mix, 1 µL cDNA, and 10 µL SYBR Green. Plates were run in the PCR machine at 40 cycles with the following parameters: 94º C for 2 s, 60º C for 30 s and 72º C for 30 s. miRNA expression is normalized to Gapdh. The quantification method applied for analysis is known as Delta Delta CT, which is an approximation method that corrects for baseline expression of the standard gene, Gapdh in this case.

miRNA Target Prediction

Both experimentally verified and predicted miRNA targets were compiled using an online software miRWalk (http://www.ma.uni-heidelberg.de/apps/zmf/mirwalk). Verified

targets are identified through Pubmed searches. Prediction of miRNA targets relies on internal algorithms created by mirWalk in addition to comparison with other target prediction software. In this analysis, only miRNA targets that were predicted by three different algorithms were further assessed. The three different algorithms software utilized includes; mirWalk, miRanda, and miRDB. The expression values for these genes were then identified through search of the transcriptome dataset comparing expression between WT and Cit-K$^{fh/fh}$. Fold regulation between -1.1 and 1.1 is denoted as no change, above 1.1 is up regulated, and below 1.1 is down regulated.

GENEMANIA Network Analysis

Network analysis was completed by insertion of all up-regulated miRNA targets with greater than 1.2 fold up-regulation in the RNA-Seq dataset into GENEMANIA. Parameters for network creation are as follow: database set to genes in human, selection of 50 related genes, and physical interactions only.

Supplemental Information

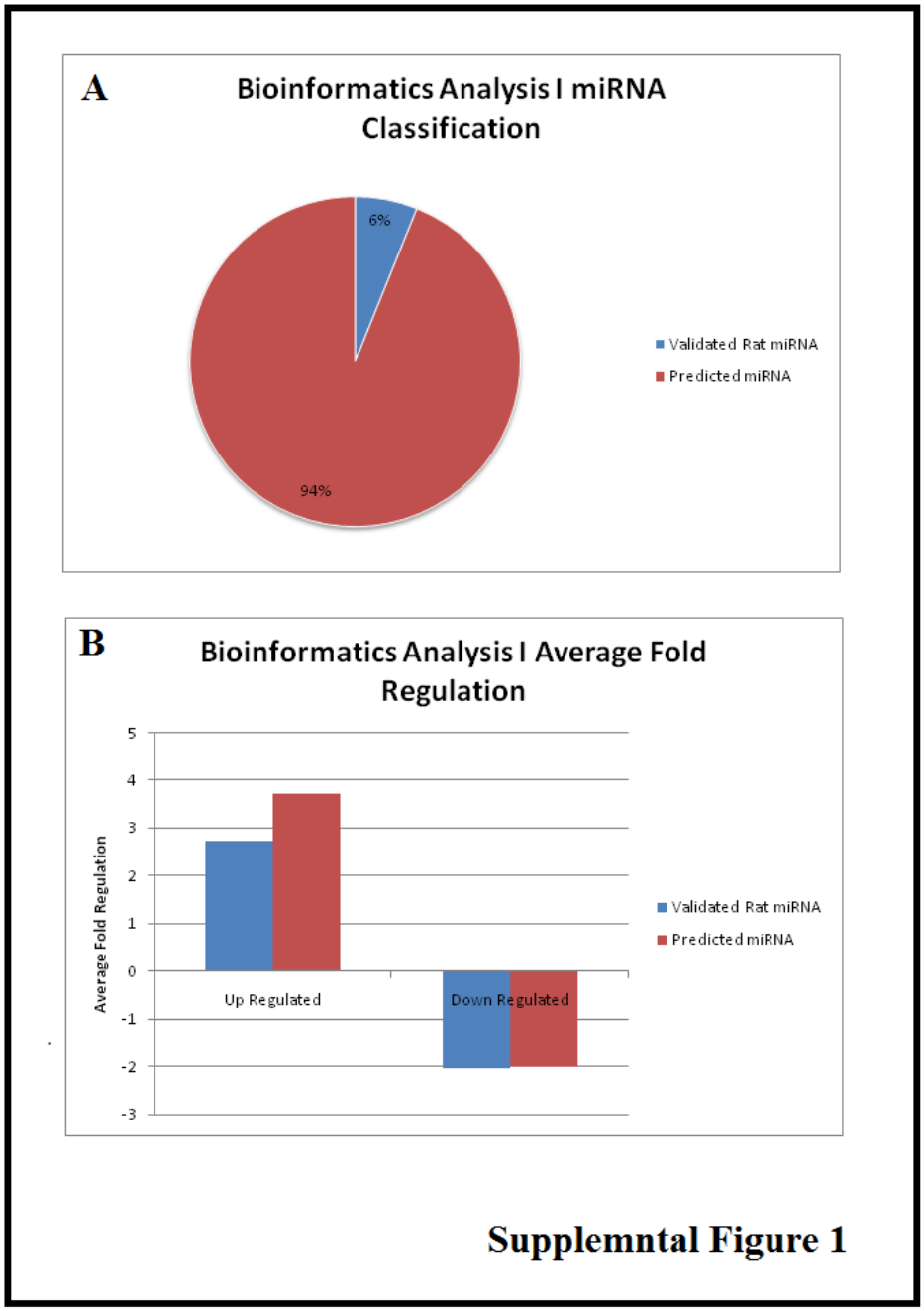

Supplemental Figure 1. Bioinformatics Analyses of Cit-K$^{fh/fh}$ RNA-Seq Dataset.

Analysis I consisted of blasting intergenic reads against all mature miRNA sequences. N=3.

A) The pie chart illustrates the percentage of detected miRNAs that are either validated in rat or are predicted based on other species. Analysis I detected a total of 82 miRNAs with greater than 10 reads between the replicates of either WT or Cit-K$^{fh/fh}$.

B) A bar graph revealing the average fold regulation of validated rat miRNAs and predicted miRNAs. Average fold regulation is separated between up-regulated and down-regulated miRNAs. Average fold regulation is the average of the ratios of $2^{\Delta\Delta CT}$ between WT and Cit-$K^{fh/fh}$ for all miRNAs in that specific category.

Analysis I Explanation

Analysis I was completed by blasting all unique intergenic sequences detected by RNA-Seq against confirmed miRNAs found across all species in mirBASE. Homology between the 35 nucleotide read and the 18-22 nucleotide mature miRNA sequence resulted in the annotation of that read as a miRNA. However, the aligned reads that were identified as miRNAs were never matched to the actual genomic location of their respective matched miRNA. Evaluation of genomic locations given for annotated miRNAs through this analysis showed no match with the actual genomic location of them miRNA. This analysis is therefore erroneous and cannot be used to accurately provide information on the expression of miRNAs in the Cit-$K^{fh/fh}$.

Analysis I (Sup. Fig. 1A) revealed expression of 82 primary-miRNAs, 5 of which were experimentally verified miRNAs found in rattus, and 77 of which had been predicted based on miRNAs present in other species. Of the 5 experimentally verified miRNAs, rno-mir-466b, rno-mir-370, and rno-mir-207 were detected in this analysis. Further analysis of this data was completed to identify differential expression of detected miRNAs in the Cit-$K^{fh/fh}$. Results indicate an average fold expression (Sup. Fig. 1B) of 2.72 and 3.72 for up-regulated miRNAs, which fall under the category of validated in rattus and predicted respectively. Average fold regulation of down regulated miRNAs did not vary significantly, with -2.01 for validated and -2.00 for predicted miRNAs.

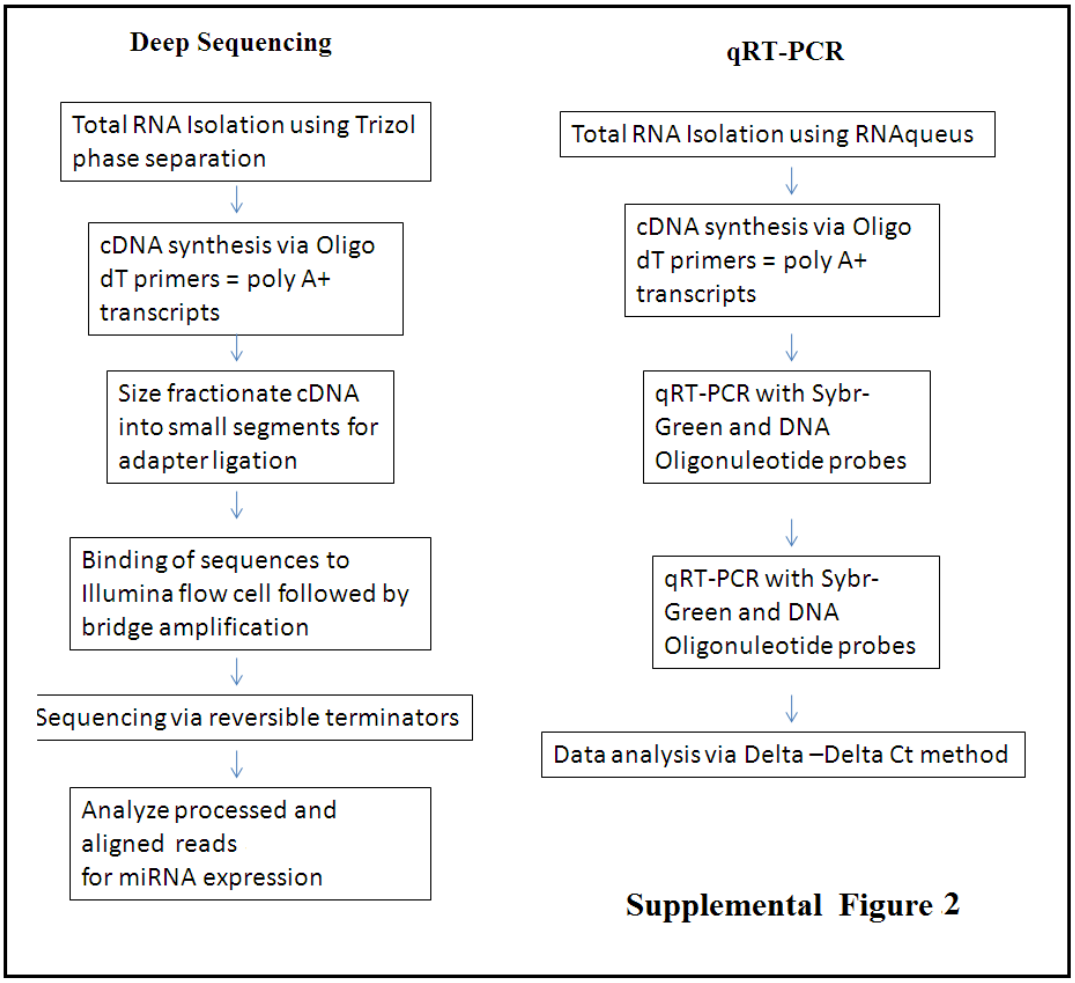

Supplemental Figure 2. Flowchart for experimental procedure.

Procedure for both the basics of how RNA-Seq and qRT-PCR was completed. See methods for details.

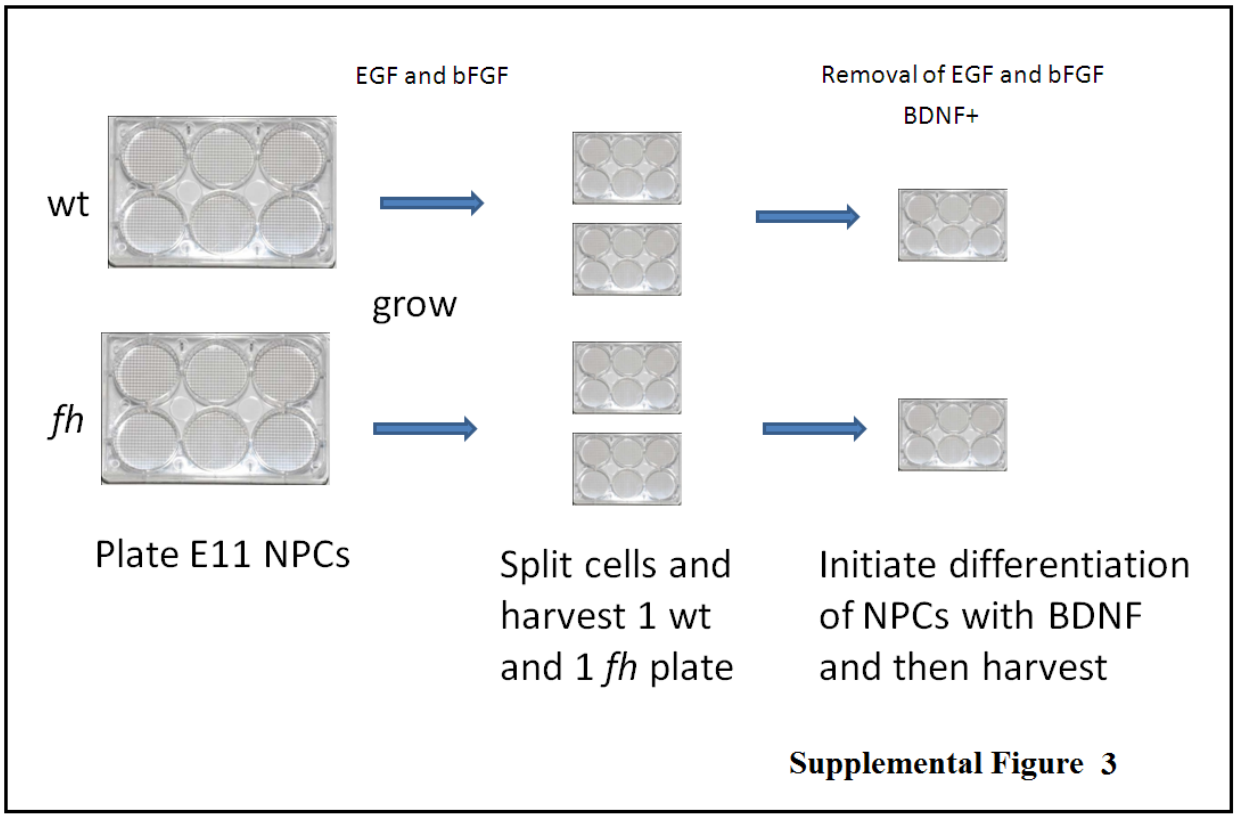

Supplemental Figure 3. Experimental procedure for the in-vitro model to mimic the onset of differentiation

See methods for details.

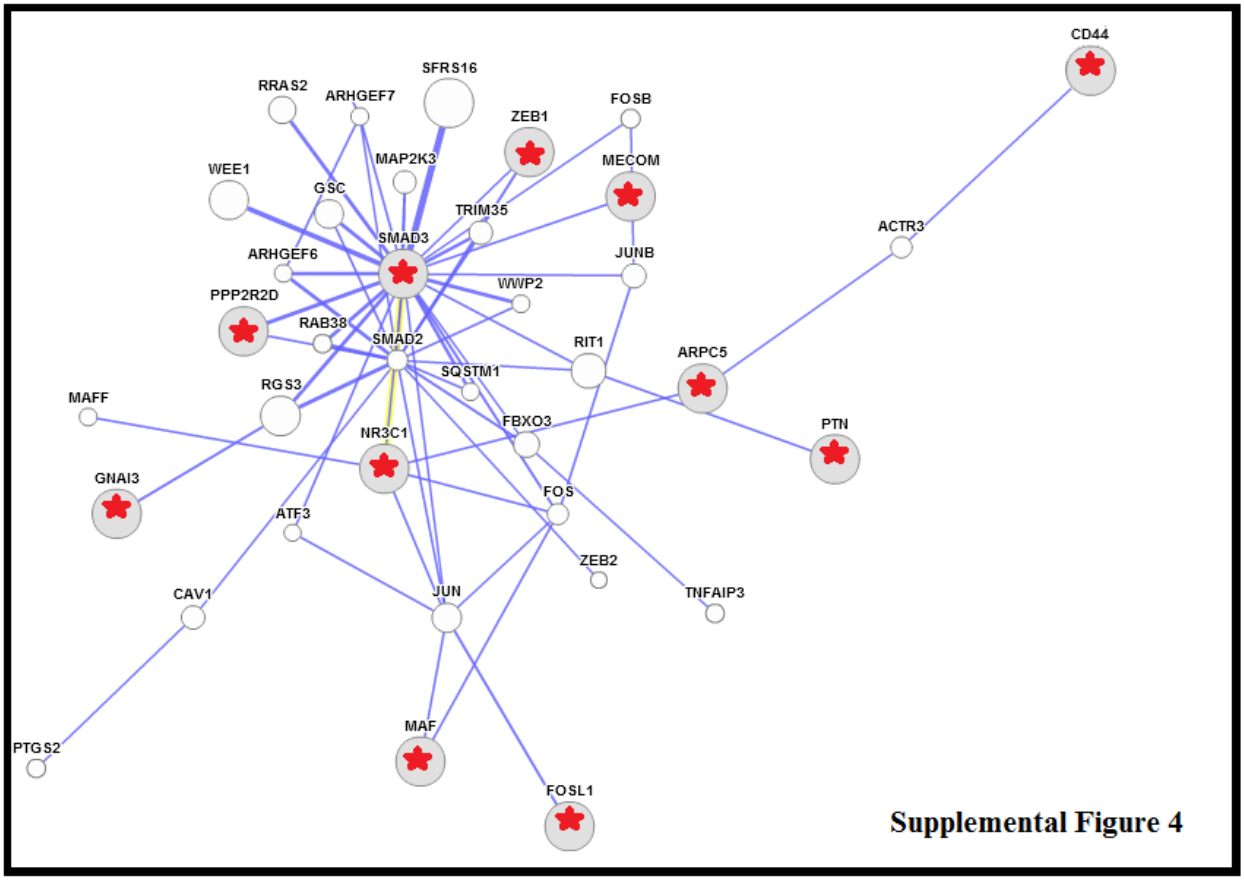

Supplemental Figure 4. GENEMANIA Regulatory network

Genemania analysis of all predicted targets that were up regulated greater than 1.2 fold in the RNA-Seq dataset resulted in a regulatory network that converges on SMAD3. Five (ZEB1, MECOM, PPPR2D, PTN, and NR3C1) of the up-regulated miRNA targets directly interact with SMAD3, in addition to two genes (FOSL1 and MAF) that indirectly regulate SMAD3 through a converging interaction with Jun.

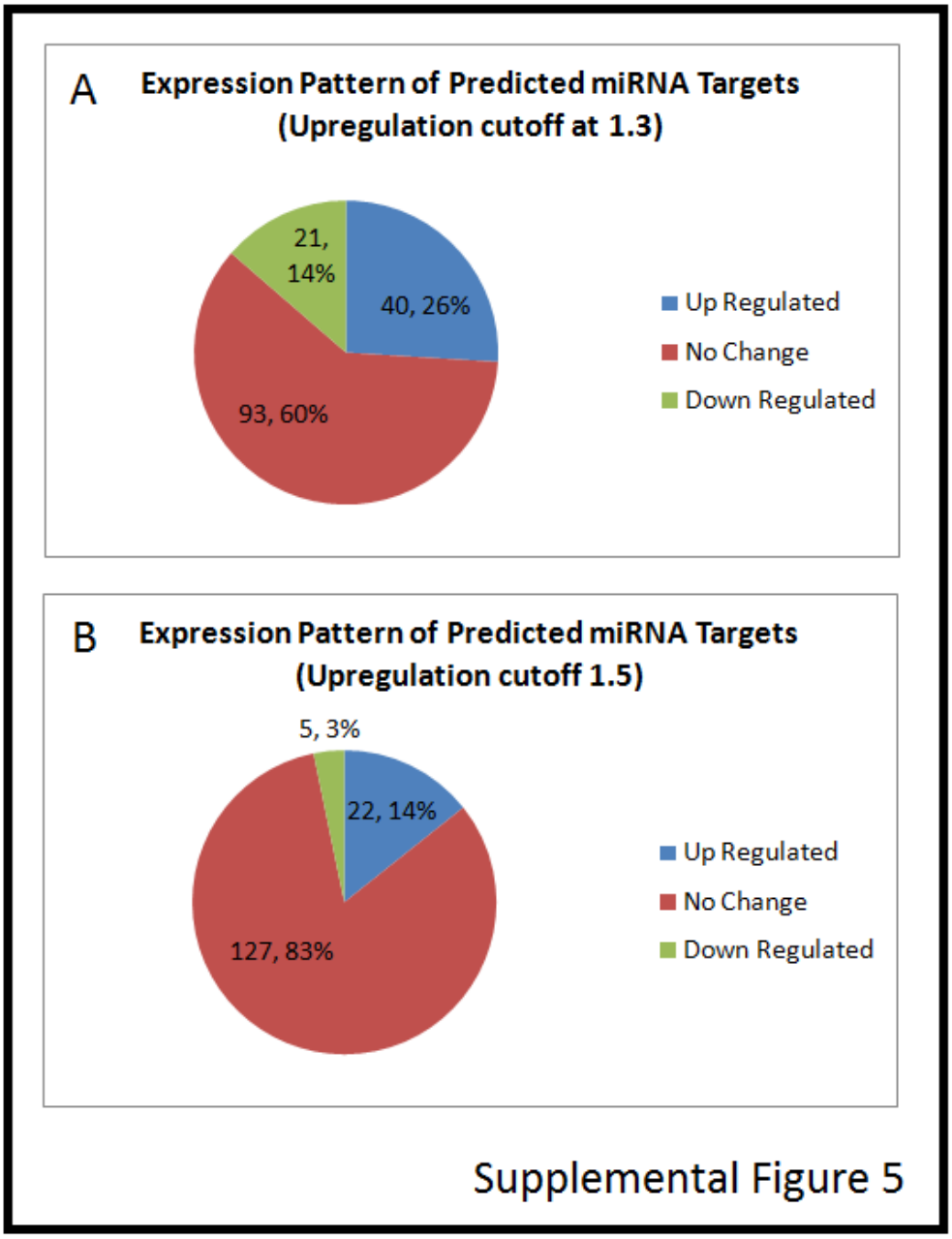

Supplemental Figure 5 Expression Pattern of Predicted miRNA Targets at different thresholds for fold regulation.

- **A.** The threshold for up regulation was held at 1.3 and down regulation at -1.3. This difference in streingency resulted in a decrease in the percent of up regulated transcripts, but remained at a percentage greater than in the Cit-K$^{fh/fh}$ transcriptome analysis.
- **B.** At a threshold of 1.5/-1.5 for up and down regulation respectively, there were still a greater percentage of up regulated transcripts.

A **Table 1**

miRNA	Left Primer	Right Primer
Rno-mir-207	CTTGCGCTTCTCCTGGCTCTC	ACCTGGCGCCGACCGTTAAG
Rno-mir-370	GAGACCAGGTCACGTCTCTGC	GGCACCTGAGTGATGGTGATAG
Rno-mir-22	CTGGCTGAGCCGCAGTAGTTC	TCTTCCTCCTCGAAGCCAGTG
Rno-mir-466b	TGCTTGCACGTGTGTGTATGTG	TGGCAAGCACTTGGTAGACAG

B

Query: 1-21 rno-mir-207 : 46-66 score: 105 evalue: 0.003

```
UserSeq          1  cuugcgcuucuccuggcucuc  21
                    |||||||||||||||||||||
rno-mir-207     46  cuugcgcuucuccuggcucuc  66
```

Query: 1-21 mmu-mir-370 : 8-28 score: 105 evalue: 0.003

```
UserSeq          1  gagaccaggucacgucucugc  21
                    ||||||||||||||||||||
mmu-mir-370      8  gagaccaggucacgucucugc  28
```

Query: 1-21 rno-mir-22 : 3-23 score: 105 evalue: 0.003

```
UserSeq          1  cuggcugagccgcaguaguuc  21
                    |||||||||||||||||||||
rno-mir-22       3  cuggcugagccgcaguaguuc  23
```

Query: 1-22 rno-mir-466b-1 : 59-80 score: 110 evalue: 0.001

```
UserSeq         22  ugcuugcacguguguguaugug  1
                    ||||||||||||||||||||||
rno-mir-466b-1  59  ugcuugcacguguguguaugug  80
```

Table 1. Primer Validation

A) Left and right primer sequences which were used to qRTPCR amplification of primary-miRNAs
B) Blast results of the left primer sequence against miRBase for validation of primer homology to specified miRNA sequence.

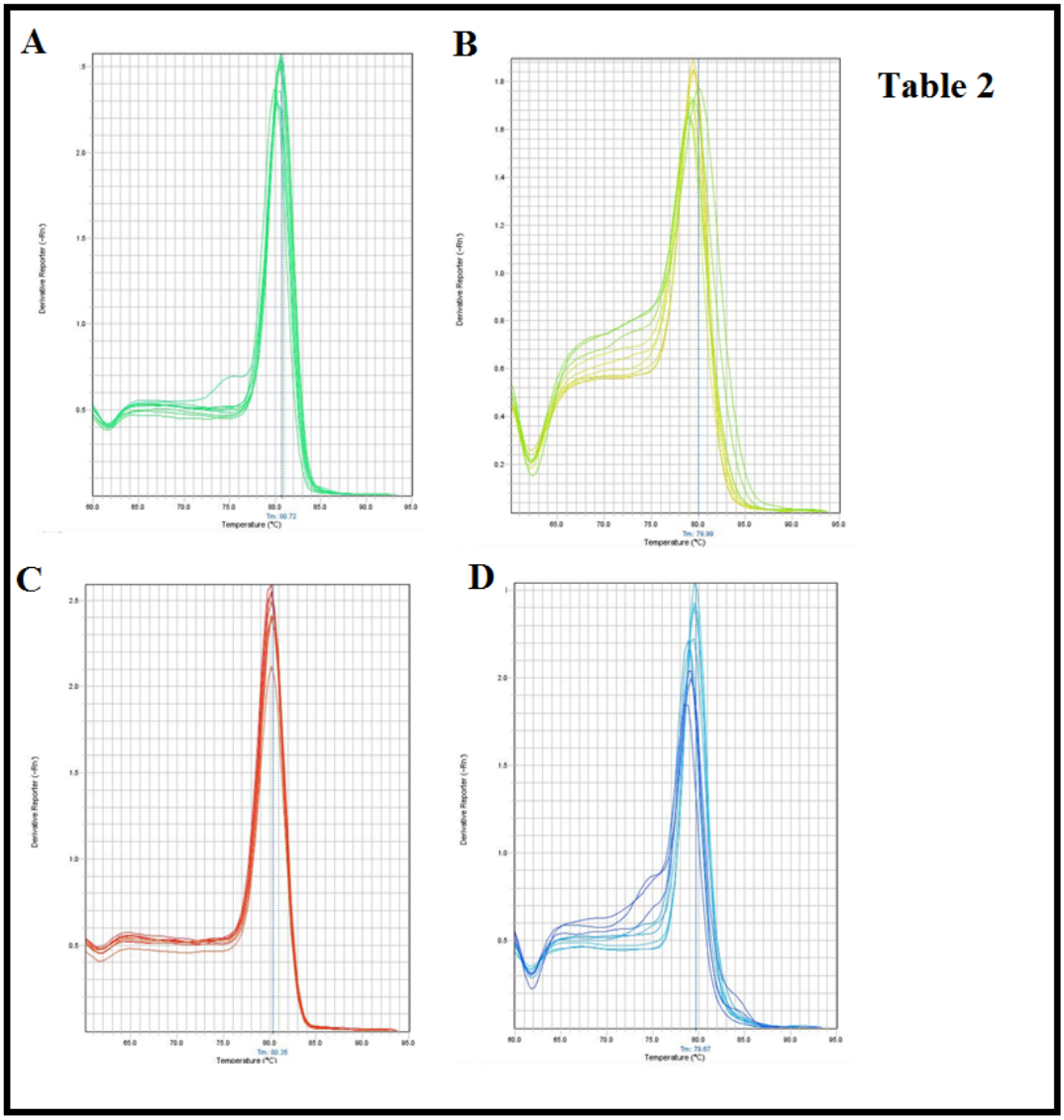

Table 2. Melt Curve for verification of no contamination and amplification of one product during qRTPCR

A) Melt curve for rno-mir-207
B) Melt curve for rno-mir-22
C) Melt curve for rno-mir-370
D) Melt curve for rno-mir-466b

qRT-PCR Data for Passage 3 NPCs

Sample	miRNA	Raw Ct	Ct Normalized to Gapdh
np 1.1 wt	mir 207	26.10663	6.34560585
np 1.1 wt	mir 207	26.08096	6.319936752
np 1.1 wt	mir 207	26.2233	6.462276459
np 2.1 wt	mir 207	25.67423	7.519083023
np 2.1 wt	mir 207	25.35311	7.197961807
np 2.1 wt	mir 207	25.4258	7.270656586
np 1.1 fh	mir 207	25.68637	6.784425735
np 1.1 fh	mir 207	25.74408	6.842142105
np 1.1 fh	mir 207	25.62185	6.719909668
np 2.1 fh	mir 207	24.77232	7.117351532
np 2.1 fh	mir 207	24.932	7.277038574
np 2.1 fh	mir 207	25.04158	7.386615753
np 1.1 wt	mir 370	31.8703	12.10927963
np 1.1 wt	mir 370	31.92088	12.15985107
np 1.1 wt	mir 370	32.18364	12.42261887
np 2.1 wt	mir 370	29.66167	11.50652695
np 2.1 wt	mir 370	29.51004	11.35489845
np 2.1 wt	mir 370	29.39007	11.23492432
np 1.1 fh	mir 370	33.78157	14.87962723
np 1.1 fh	mir 370	33.38417	14.48223114
np 1.1 fh	mir 370	33.13159	14.2296524
np 2.1 fh	mir 370	32.66386	15.00889587
np 2.1 fh	mir 370	32.46123	14.80626297
np 2.1 fh	mir 370	32.41951	14.76454544
np 1.1 wt	mir 22	28.05457	8.293544769
np 1.1 wt	mir 22	28.13369	8.372661591
np 1.1 wt	mir 22	28.12456	8.363538742
np 2.1 wt	mir 22	26.82002	8.664873123
np 2.1 wt	mir 22	26.92597	8.770830154
np 2.1 wt	mir 22	26.91131	8.756162643
np 1.1 fh	mir 22	27.86877	8.966835022
np 1.1 fh	mir 22	27.79559	8.893651962
np 1.1 fh	mir 22	27.68649	8.784549713
np 2.1 fh	mir 22	27.85853	10.20356941
np 2.1 fh	mir 22	27.81175	10.15678978
np 2.1 fh	mir 22	27.53199	9.877023697

qRT-PCR Data for Passage 3 Forebrain Lysate

Sample	miRNA	Raw Ct	Ct Normalized to Gapdh
wt 3.2	mir 207	24.48234	5.599285126
wt 3.2	mir 207	24.44692	5.563865662
wt 3.2	mir 207	24.7318	5.848752975
wt 4.2	mir 207	24.58825	5.61570549
wt 4.2	mir 207	24.75125	5.778705597
wt 4.2	mir 207	24.85486	5.882316589
fh 17.2	mir 207	23.78473	5.714248657
fh 17.2	mir 207	23.80448	5.734003067
fh 17.2	mir 207	23.84203	5.771551132
fh 13	mir 207	23.90849	6.487796783
fh 13	mir 207	24.25699	6.836301804
fh 13	mir 207	24.29796	6.877267838
wt 3.2	mir 370	29.37197	10.4889183
wt 3.2	mir 370	29.52237	10.63931847
wt 3.2	mir 370	29.54372	10.66067123
wt 4.2	mir 370	29.58916	10.6166153
wt 4.2	mir 370	29.75958	10.78703499
wt 4.2	mir 370	29.69665	10.72410393
fh 13	mir 370	29.0812	11.01072502
fh 13	mir 370	29.24919	11.17871475
fh 13	mir 370	29.26663	11.19615364
fh 17.2	mir 370	28.83652	11.4158268
fh 17.2	mir 370	28.91521	11.49451637
fh 17.2	mir 370	28.94327	11.52257729
wt 3.2	mir 22	27.1597	8.27665329
wt 3.2	mir 22	26.96443	8.081382751
wt 3.2	mir 22	27.79917	8.916122437
wt 4.2	mir 22	27.50676	8.534221649
wt 4.2	mir 22	27.32773	8.35518837
wt 4.2	mir 22	27.2818	8.3092556
fh 13	mir 22	27.11379	9.043308258
fh 13	mir 22	26.88375	8.813270569
fh 13	mir 22	26.91553	8.845050812
fh 17.2	mir 22	26.88216	9.461473465
fh 17.2	mir 22	26.65228	9.231588364
fh 17.2	mir 22	26.3473	8.926612854

qRT-PCR Data for Passage 1 NPCs and MFBCs

Sample	miRNA	Raw ct	Norm to Gapdh	Sample	miRNA	Raw ct	Norm to Gapdh
wt1	466b	32.9250641	14.4947777	dwt	466b	31.5982208	13.1058922
wt2	466b	32.3158913	13.9330826	dwt2	466b	32.9237556	13.8046665
wt3	466b	32.5224762	14.0389519	dwt3	466b	32.5798759	13.4607868
fh1	466b	31.8561134	13.4576855	dfh1	466b	33.4149742	15.4769382
fh2	466b	31.897234	13.5546093	dfh2	466b	33.4049339	14.8518753
X	X	X	X	dfh3	466b	33.5549774	15.3428612
wt1	207	26.9332314	8.50294495	dwt	207	26.1925507	7.70022202
wt2	207	27.2862492	8.90344048	dwt2	207	26.6112957	7.83275223
wt3	207	27.1718311	8.68830681	dwt3	207	26.9638538	7.84476471
fh1	207	27.4136715	9.01524353	dfh1	207	26.8842907	8.94625473
fh2	207	27.3698082	9.02718353	dfh2	207	27.5241718	8.9711132
X	X	X	X	dfh3	207	26.9167347	8.70461845
wt1	370	32.0322762	13.6019897	dwt	370	31.2241154	12.7317867
wt2	370	32.0543671	13.6715584	dwt2	370	32.6124191	13.8338757
wt3	370	31.9723339	13.4888096	dwt3	370	31.6141491	12.49506
fh1	370	31.9080315	13.5096035	dfh1	370	32.4628334	14.5247974
fh2	370	32.2079697	13.865345	dfh2	370	32.5295715	13.9765129
X	X	X	X	dfh3	370	33.0387421	14.8266258

Sample	miRNA	Raw ct	Norm to Gapdh	Sample	miRNA	Raw ct	Norm to Gapdh
wt1	mir22	28.7962666	10.3659801	dwt	mir22	27.4863148	8.99398613
wt2	mir22	28.7932625	10.4104538	dwt2	mir22	28.1286526	9.3501091
wt3	mir22	28.8736401	10.3901157	dwt3	mir22	28.4315491	9.31245995
fh1	mir22	28.5243549	10.125927	dfh1	mir22	27.8337135	9.89567757
fh2	mir22	28.7104607	10.367836	dfh2	mir22	28.2987671	9.74570847
X	X	X	X	dfh3	mir22	27.8743248	9.66220856
wt1	mir370	32.2765808	13.8462944	dwt	mir370	30.9146061	12.4222775
wt2	mir370	31.5366554	13.1538467	dwt2	mir370	31.7274742	12.9489307
wt3	mir370	31.5673981	13.0838737	dwt3	mir370	31.7956295	12.6765404
fh1	mir370	31.4048901	13.0064621	dfh1	mir370	31.8144569	13.876421
fh2	mir370	31.6305447	13.28792	dfh2	mir370	32.1154594	13.5624008
X	X	X	X	dfh3	mir370	32.1343994	13.9222832

miRNA Predicted Targets Data

Up regulation/Down regulation Cut off= 1.1/-1.1

RAW		Up Reg	No Change	Down Reg	TOTAL	PERCENT		Up Reg	No Change	Down Reg
	mir-370	16	7	8	31		**mir-370**	0.516129	0.225806	0.258065
	mir207	21	9	9	39		**mir207**	0.538462	0.230769	0.230769
	mir466b	24	11	10	45		**mir466b**	0.533333	0.244444	0.222222
	mir22	17	12	10	39		**mir22**	0.435897	0.307692	0.25641
	TOTAL	78	39	37	154		**total**	0.506494	0.253247	0.24026

Up regulation/Down regulation Cut off= 1.3/-1.3

RAW		Up Reg	No Change	Down Reg	TOTAL	Percent	Up Reg	No Change	Down Reg
	mir-370	4	24	3	31		0.129032	0.774194	0.096774
	mir207	9	27	3	39		0.230769	0.692308	0.076923
	mir466b	18	17	10	45		0.4	0.377778	0.222222
	mir22	9	25	5	39		0.230769	0.641026	0.128205
	TOTAL	40	93	21	154		0.25974	0.603896	0.136364

Up regulation/Down regulation Cut off= 1.5/-1.5

RAW		Up Reg	No Change	Down Reg	TOTAL	Percent	Up Reg	No Change	Down Reg
	mir-370	3	26	2	31		0.096774	0.83871	0.064516
	mir207	6	32	1	39		0.153846	0.820513	0.025641
	mir466b	10	34	1	45		0.222222	0.755556	0.022222
	mir22	3	35	1	39		0.076923	0.897436	0.025641
	TOTAL	22	127	5	154		0.142857	0.824675	0.032468

mir 22			mir 370			mir-466b			mir-207		
Arpc5	1.98	up	Fas	1.75	up	Slc24a2	2.32	up	Fut7	2.05	up
Nr3c1	1.87	up	Rfx3	1.55	up	Has2	1.966	up	Cd44	1.98	up
Klf6	1.57	up	Sele	1.51	up	Slc31a2	1.89	up	Nr3c1	1.87	up
Ddit4	1.47	up	Yipf1	1.33	up	Nr3c1	1.87	up	Gcnt1	1.71	up
Aip1	1.35	up	Abcd2	1.24	up	Gpm6a	1.8	up	Gtpbp8	1.69	up
Tmed5	1.34	up	Fosl1	1.22	up	Cd24	1.72	up	Nphs1	1.52	up
Emp1	1.34	up	Dgat2	1.216	up	Slc2a13	1.622	up	Kcnd2	1.46	up
Mecom	1.33	up	Cpt1a	1.2	up	Maf	1.58	up	Ptn	1.43	up
Htr2c	1.31	up	Zeb1	1.2	up	Nphs1	1.52	up	Ppm1b	1.31	up
Gnai3	1.28	up	Laptm5	1.18	up	Elovl6	1.51	up	Ppp2r2d	1.29	up
Tor3a	1.27	up	Mapre1	1.18	up	Tcea1	1.49	up	Cldnd1	1.28	up
Cldnd1	1.23	up	Slc27a1	1.16	up	Gabrb3	1.45	up	Tcf12	1.256	up
Cspg4	1.2	up	Klhl24	1.16	up	Kcnq3	1.43	up	Prkag1	1.24	up
Pomc	1.14	up	Vamp1	1.16	up	Selt	1.42	up	Pkia	1.22	up
Btg1	1.14	up	Atp5c1	1.113	up	Hsd17b12	1.39	up	Smad3	1.22	up
Arfip2	1.13	up	Bhlhb8	1.11	up	Acsl4	1.38	up	Npr1	1.2	up
Ppara	1.11	up	Tgfbr2	1.1	no change	Sfxn2	1.38	up	Igsf6	1.18	up
Wrnip1	1.095	no change	Snapap	1.08	no change	Kcnv1	1.32	up	Strap	1.179	up
Nudt4	1.04	no change	Lkap	1.05	no change	Pex3	1.27	up	Dnajb11	1.13	up
Mcm7	1.02	no change	Ap3m1	1.04	no change	Ctsd	1.25	up	Ppap2b	1.12	up
Ets1	1.008	no change	Zfhx1b	-1.015	no change	Rbm34	1.21	up	Tmem33	1.11	up
Pten	-1.009	no change	Gpd1	-1.03	no change	Prnp	1.14	up	Rpn2	1.08	no change
Yars	-1.01	no change	Raf1	-1.05	no change	Khdrbs2	1.13	up	Epb4.1l1	1.04	no change
Trub1	-1.01	no change	Hirip3	-1.14	down	Rbl2	1.11	up	Slco2b1	1.03	no change
Ephb1	-1.05	no change	Zfp111	-1.16	down	Rgs4	1.09	no change	Epn2	-1.023	no change
H3f3b	-1.05	no change	Ing3	-1.18	down	Crcp	1.008	no change	Nr5a2	-1.06	no change
Frap1	-1.06	no change	Pla2g2c	-1.2	down	Enpp5	-1.01	no change	Mageh1	-1.06	no change

Slc9a5	-1.08	no change	Inpp4a	-1.25	down	Zhx1	-1.02	no change	Aqp4	-1.07	no change
Sv2a	-1.14	no change	Emp2	-1.3	down	Vsnl1	-1.03	no change	Dap	-1.07	no change
Rab26	-1.2	down	Map3k8	-2.21	down	Extl3	-1.05	no change	Slc9a5	-1.08	no change
Max	-1.22	down	Dnali1	-2.72	down	Dclk1	-1.06	no change	Pim1	-1.15	down
Myst2	-1.22	down				Lmcd1	-1.08	no change	Myd88	-1.2	down
Net1	-1.23	down				Mafk	-1.08	no change	Slc22a12	-1.2	down
Podxl	-1.27	down				Sv2a	-1.1	no change	Bicd2	-1.21	down
Ankrd13	-1.31	down				G4	-1.1	no change	Cnot4	-1.24	down
Pdap1	-1.33	down				Trim39	-1.11	down	Tm2d2	-1.28	down
Slc6a1	-1.38	down				Stambp	-1.15	down	Sc5d	-1.31	down
Cav3	-1.45	down				Cat	-1.16	down	Impg2	-1.39	down
Myc	-1.55	down				Slc25a10	-1.2	down	Kcna4	-3.43	down
						Rab7	-1.2	down			
						Cyb5r3	-1.23	down			
						Net1	-1.23	down			
						Ceacam1	-1.29	down			
						Nlgn3	-1.39	down			
						Ret	-2.13	down			

References

1. Sarkisian, M.R., Li, W., Di Cunto, F., D'Mello, S.R. & LoTurco, J.J. Citron-kinase, a protein essential to cytokinesis in neuronal progenitors, is deleted in the flathead mutant rat. *J. Neurosci* **22**, RC217 (2002).

2. Sweeney, S.J., Campbell, P. & Bosco, G. Drosophila sticky/citron kinase is a regulator of cell-cycle progression, genetically interacts with Argonaute 1 and modulates epigenetic gene silencing. *Genetics* **178**, 1311-1325 (2008).
3. De Pietri Tonelli, D. et al. miRNAs are essential for survival and differentiation of newborn neurons but not for expansion of neural progenitors during early neurogenesis in the mouse embryonic neocortex. *Development* **135**, 3911-3921 (2008).
4. LoTurco, J.J., Patel, K., LaPierre, P. Girgenti, M.J. Phosphorylation by citron kinase creates a chromatin state required for neural progenitor self-renewal. Program No. 233.70. 2010 Neuroscience Meeting Planner. San Diego, CA: Society for Neuroscience, 2010.
5. LoTurco, J.J., Sarkisian, M.R., Cosker, L. & Bai, J. Citron kinase is a regulator of mitosis and neurogenic cytokinesis in the neocortical ventricular zone. *Cereb. Cortex* **13**, 588-591 (2003).
6. Perruisseau-Carrier, C., Jurga, M., Forraz, N. & McGuckin, C.P. miRNAs Stem Cell Reprogramming for Neuronal Induction and Differentiation. *Mol. Neurobiol* **43**, 215-227 (2011).
7. Zhao, C., Sun, G., Li, S. & Shi, Y. A feedback regulatory loop involving microRNA-9 and nuclear receptor TLX in neural stem cell fate determination. *Nat. Struct. Mol. Biol* **16**, 365-371 (2009).
8. Lau, P. & Hudson, L.D. MicroRNAs in neural cell differentiation. *Brain Res* **1338**, 14-19 (2010).
9. Liu, C. & Zhao, X. MicroRNAs in adult and embryonic neurogenesis. *Neuromolecular Med* **11**, 141-152 (2009).
10. Shi, Y. et al. MicroRNA regulation of neural stem cells and neurogenesis. *J. Neurosci* **30**, 14931-14936 (2010).
11. Liu, C. et al. Epigenetic regulation of miR-184 by MBD1 governs neural stem cell proliferation and differentiation. *Cell Stem Cell* **6**, 433-444 (2010).
12. Newman, M.A. & Hammond, S.M. Emerging paradigms of regulated microRNA processing. *Genes Dev* **24**, 1086-1092 (2010).
13. Slezak-Prochazka, I., Durmus, S., Kroesen, B.-J. & van den Berg, A. MicroRNAs, macrocontrol: regulation of miRNA processing. *RNA* **16**, 1087-1095 (2010).
14. Siomi, H. & Siomi, M.C. Posttranscriptional regulation of microRNA biogenesis in animals. *Mol. Cell* **38**, 323-332 (2010).
15. Davis-Dusenbery, B.N. & Hata, A. Mechanisms of control of microRNA biogenesis. *J. Biochem* **148**, 381-392 (2010).
16. Iwasaki, S., Kawamata, T. & Tomari, Y. Drosophila Argonaute1 and Argonaute2 Employ Distinct Mechanisms for Translational Repression. *Molecular Cell* **34**, 58-67 (2009).
17. Guo, H., Ingolia, N.T., Weissman, J.S. & Bartel, D.P. Mammalian microRNAs predominantly act to decrease target mRNA levels. *Nature* **466**, 835-840 (2010).
18. Lewis, B.P., Shih, I.-hung, Jones-Rhoades, M.W., Bartel, D.P. & Burge, C.B. Prediction of mammalian microRNA targets. *Cell* **115**, 787-798 (2003).

19. Silva, A., Pereira, J., Oliveira, C.R., Relvas, J.B. & Rego, A.C. BDNF and extracellular matrix regulate differentiation of mice neurosphere-derived cells into a GABAergic neuronal phenotype. *J. Neurosci. Res* **87**, 1986-1996 (2009).
20. Li, T., Jiang, L., Zhang, X. & Chen, H. In-vitro effects of brain-derived neurotrophic factor on neural progenitor/stem cells from rat hippocampus. *Neuroreport* **20**, 295-300 (2009).
21. Raff, M. Intracellular developmental timers. *Cold Spring Harb. Symp. Quant. Biol* **72**, 431-435 (2007).
22. Vazin, T. et al. A novel combination of factors, termed SPIE, which promotes dopaminergic neuron differentiation from human embryonic stem cells. *PLoS ONE* **4**, e6606 (2009).
23. Dweep, H., Sticht, C., Pandey, P., Gretz, N., miRWalk - database: prediction of possible miRNA binding sites by "walking" the genes of 3 genomes, Journal of Biomedical Informatics (2011), doi: 10.1016/ j.jbi.2011.05.002
24. Postigo, A.A., Depp, J.L., Taylor, J.J. & Kroll, K.L. Regulation of Smad signaling through a differential recruitment of coactivators and corepressors by ZEB proteins. *EMBO J* **22**, 2453-2462 (2003)
25. Song, C.-Z., Tian, X. & Gelehrter, T.D. Glucocorticoid receptor inhibits transforming growth factor-β signaling by directly targeting the transcriptional activation function of Smad3. *Proceedings of the National Academy of Sciences* **96**, 11776 -11781 (1999).
26. Park, T.J. et al. Pleiotrophin inhibits transforming growth factor β1-induced apoptosis in hepatoma cell lines. *Molecular Carcinogenesis* **47**, 784-796 (2008).
27. Furumatsu, T. & Asahara, H. Histone acetylation influences the activity of Sox9-related transcriptional complex. *Acta Med. Okayama* **64**, 351-357 (2010).
28. García-Campmany, L. & Martí, E. The TGFbeta intracellular effector Smad3 regulates neuronal differentiation and cell fate specification in the developing spinal cord. *Development* **134**, 65-75 (2007).
29. Izutsu, K. et al. The co repressor CtBP interacts with Evi-1 to repress transforming growth factor β signaling. *Blood* **97**, 2815 -2822 (2001).
30. Batut, J. et al. Two highly related regulatory subunits of PP2A exert opposite effects on TGF-beta/Activin/Nodal signaling. *Development* **135**, 2927-2937 (2008).
31. Abney, E.R., Bartlett, P.P. & Raff, M.C. Astrocytes, ependymal cells, and oligodendrocytes develop on schedule in dissociated cell cultures of embryonic rat brain. *Developmental Biology* **83**, 301-310 (1981).